Ref.TH.3244-CERN

PHENOMENOLOGY OF PHOTON-$e^{\pm}$ COLLISIONS

F.M. Renard

CERN -- Geneva

ABSTRACT

The physical interest of $\gamma e^{\pm}$ collisions is examined. A basic formalism is established. Cross-sections are computed with general couplings and polarization states. Illustrations are given for QED tests, Z^0 and $W^{\pm}$ production, various electro-weak processes including $\gamma\gamma$ collisions and the search for new currents and particles.

Ref.TH.3244-CERN
12 February 1982

1. - INTRODUCTION

The possibility of carrying out direct $\gamma e^{\pm}$ collisions at the Stanford Linear Collider (SLC) has recently been noticed[1]. It is proposed to use a laser beam (with energy $E_\gamma \lesssim 5$ eV) in order to produce an intense and high energy ($E_\gamma \lesssim 40$ GeV) photon beam from backward Compton scattering on one $e^{\mp}$ bunch of the SLC. This second photon beam then interacts with the $e^{\pm}$ bunch going in the opposite direction ($E_e \simeq 50$ GeV) so one gets $\gamma e^{\pm}$ collisions with total energy $\sqrt{s} \lesssim 90$ GeV in their centre-of-mass. The luminosity is expected to be only slightly weaker than the designed e^+e^- luminosity of the SLC, i.e., of the order of 10^{30} cm^{-2} sec^{-1}.

This should be compared with another way of doing $\gamma e^{\pm}$ collisions, i.e., e^+e^- inelastic scattering with quasi-real photon exchange (Fig. 1); in this case the effective luminosity is the product of the luminosity L of the e^+e^- storage ring times the quasi-real emission factor K. With $L \simeq 10^{31}$ to 10^{32} cm^{-2} sec^{-1} and $\langle K(E,z)\rangle \simeq 10^{-1}$ for $E = 2E_e \simeq 100$ to 200 GeV and $z = \sqrt{s}/E \simeq$ $\simeq 1/2$ one gets an effective $\gamma e^{\pm}$ luminosity at least comparable to the above one. However, a realistic comparison should take into account detection efficiency and background problems which depend on the kinematics of each channel that one wants to study. Direct $\gamma e^{\pm}$ collisions may appear more appealing because of their simpler kinematics.

Independently of the device to be used, the physics of $\gamma e^{\pm}$ collisions is very interesting. One would have new ways of studying the behaviour of electron and photon interactions at high energies, the deep structure of electroweak interactions and the possibility of new currents and new particles.

First there are well-known reactions like Compton scattering or lepton pair production which provide interesting tests of QED in kinematical domains which have not yet been explored, being different from those accessible in e^+e^- annihilation. For example, one can study the behaviour of the electron propagator in the (s channel) time-like region; one can look for the formation of an excited lepton (e^*) which would appear here as a simple resonance. These QED reactions will also be useful for monitoring and for initial γ and $e^{\pm}$ polarization analysis.

Weak interactions can first be studied through the production of Z and $W^{\pm}$ bosons ($\gamma e \to Ze$ and $\gamma e \to W^{\pm}\nu_e$); as soon as $\sqrt{s} > M_Z$ or $M_{W^{\pm}}$ the cross-section is sizeable . This is especially interesting for $W^{\pm}$ production which

will be rather difficult to do in e^+e^- or hadronic collisions. $\gamma e \to W^\pm \nu_e$ also offers the possibility of studying the γWW vertex and its Yang-Mills form.

There is a large class of interesting electroweak reactions going via one boson exchange $(\gamma, Z, W^\pm)$. The simplest one with the largest cross-section is obviously the quasi-real γ exchange process that one can express in terms of $\gamma\gamma$ collisions. For this study the advantage of direct $\gamma e^\pm$ collisions with respect to e^+e^- inelastic scattering is the simpler kinematics. The bosonic state (B) coupled to $\gamma\gamma$ is produced along the incident γ direction in a simple two-body $\gamma e \to (B)e$. All the interesting features (C=+1 resonances, exotic states, boson and fermion pairs, leptons and quarks,...) looked for in $\gamma\gamma$ collisions can be observed here this way. At a lower level one has Z and $W^\pm$ processes which are also interesting to study in the form of γZ and $\gamma W^\pm$ collisions. They appear as true weak processes, but the backgrounds can be reduced if one looks for parity or charge conjugation violating terms (using $\gamma e^+/\gamma e^-$ comparisons and polarized beams).

The final and perhaps most exciting process is the hunting of new currents and new particles. There are several possibilities for them to appear here. New fermions can be formed in the direct channel or exchanged in the u channel; new bosons can be exchanged in the t channel; both of them can appear in two-body reactions $\gamma e \to B + F$. Such reactions will occur copiously if vertices like γeF, $\gamma\gamma B$, $\gamma W^\pm B^\pm$, eeB^0, eFB, $e\nu B^\pm$,... exist. There is a large set of predictions for such particles in recent models based on unified theories, supersymmetry or subconstituents. For example, one can think of neutral or charged Higgs bosons, elementary fermions and scalars, new bound states, pseudo-Goldstone bosons,... . It is very often asserted that several new phenomena, and in particular the production of new kinds of states, should appear at a scale of the order of 100 GeV (the weak interaction scale). In this energy range the electron could appear as a composite object. It is possible that some aspects of this new physics show up in $\gamma e^\pm$ collisions.

For these reasons we have thought it valuable to develop the phenomenological aspect of these collisions which have not received much attention so far. In this paper we examine systematically the list of simple reactions which can be obtained from $\gamma e^\pm$ collisions. We give the basic phenomenological tools for their description and the results for the cross-sections. These results are given in the case of polarized beams, transversally or longitudinally polarized $e^\pm$ and circularly or linearly polarized γ. We treat simultaneously the cases

of γe^- and γe^+ collisions. Many interesting effects can come out of the $\gamma e^+/\gamma e^-$ comparison with different polarization states. These results are applicable to the case of direct $\gamma e^\pm$ collisions as well as to the case of quasi-real $\gamma e^\pm$ collisions in e^+e^- inelastic scattering using the corresponding photon emission factor.

The organization of the paper is as follows. Kinematical generalities, notations and relations between inelastic e^+e^- scattering and quasi-real $\gamma e^\pm$ collisions are given in Section 2; technical details can also be found in Appendices A and B. Section 3 is devoted to QED reactions (Compton scattering, QED violations, e^* effect, lepton pair production). In Section 4 we give the cross-sections for Z^0 and $W^\pm$ production. Boson exchange processes are extensively studied in Section 5 with application to single boson and to particle pair production, particularly in the quasi-real $\gamma\gamma$ limit. In Section 6 we collect a list of simple reactions where new currents and particles can appear and we give in each case the expression of the cross-section in terms of couplings written in a rather general form.

This is obviously only a first phenomenological approach to the subject which should receive many physical and technical developments when $\gamma e^\pm$ have been planned.

2. - KINEMATICAL GENERALITIES

2a. Definitions and notations for $\gamma e^\pm$ collisions

We shall generally describe $\gamma e^\pm$ collisions in the centre-of-mass (c.m.) frame depicted in Fig. 2.

The $e^\pm$ and γ c.m. momenta are respectively:

$$\ell^\mu = (\ell^\circ, 0, 0, \ell) \qquad k^\mu = (k, 0, 0, -k)$$

with $k = \ell \simeq \ell^0$ (if $m_e \simeq 0$ is used); see Appendix A for tensorial notations and metric.

We define $s = (\ell+k)^2$ and $q^\mu = (\ell+k)^\mu = (\sqrt{s},0,0,0)$. Electron spin states are described by spinors $u(\ell,\xi)$ [and $v(\ell,\xi)$ for positrons] with the beam density matrices:

$$\rho_e = \frac{(1+\gamma^5 \not{\xi})(\not{\ell} - Q_e m_e)}{4m_e} \simeq \frac{1}{4m_e}\left[(1 - Q_e P_L \gamma^5)\not{\ell} + \gamma^5 \not{\xi}_T \not{\ell}\right] \tag{2.1}$$

$Q_e = \pm 1$ is the electric charge of $e^{\pm}$ in units of e.

The $e^{\pm}$ polarization four-vector containing longitudinal and transverse components is defined according to Fig. 2b:

$$\xi^\mu = \left(\frac{\ell}{m_e} P_L \,,\; P_T \cos\beta \,,\; P_T \sin\beta \,,\; \frac{\ell^0}{m_e} P_L\right) \tag{2.2}$$

In general we set $m_e = 0$ except in the expressions of the propagators of photon or electron exchange processes which control the forward or backward peaking of the angular distributions. Photon polarization states are described by the four-vector $\varepsilon^\mu(k,\lambda)$, with $\vec{k} \,||\, -OZ$, $\lambda = \pm 1$ being the helicity states in the c.m. frame of Fig. 2. One has:

$$\varepsilon^\mu(k,\lambda) = \frac{1}{\sqrt{2}}\left(0, \lambda, -i, 0\right)$$

Photon beam density matrices will be used in the helicity basis:

$$\rho_\gamma = \frac{1}{2}\begin{pmatrix} 1+\zeta_2 & -\zeta_3 + i\zeta_1 \\ -\zeta_3 - i\zeta_1 & 1-\zeta_2 \end{pmatrix} \tag{2.3}$$

with the Stokes vector components ζ_1 the linear polarization along $(OX \mp OY)$, $\zeta_2 \equiv \bar{\lambda}$ the mean helicity and ζ_3 the linear polarization along OX or OY. In configuration space we also use

$$E^{\mu\nu} = \varepsilon^\mu \varepsilon^{\nu *} = \frac{1}{2}\left(-g^{\mu\nu} + \frac{q^\mu q^\nu}{s} - n_3^\mu n_3^\nu\right) + \frac{\zeta_3}{2}\left(Q_{11}^{\mu\nu} - Q_{22}^{\mu\nu}\right) + \frac{\zeta_1}{2} Q_{12}^{\mu\nu} - \frac{i}{s}\zeta_2 \varepsilon^{\mu\nu\rho\sigma} k_\rho q_\sigma \tag{2.4}$$

with

$$Q_{ij}^{\mu\nu} \equiv \frac{1}{2}\left(n_i^\mu n_j^\nu + n_j^\mu n_i^\nu\right) - \frac{1}{3}\delta_{ij}\left(-g^{\mu\nu} + \frac{q^\mu q^\nu}{s}\right)$$

n_i^μ (i=1,2,3) being a three-basis of unit vectors associated with $\vec{k}$ such that $\vec{n}_1 \,||\, -OX$, $\vec{n}_2 \,||\, OY$ and $\vec{n}_3 \,||\, \vec{k} \,||\, -OZ$. So we get the helicity components:

$$E(\lambda\lambda') = \varepsilon^{\mu*}(\lambda)\varepsilon^{\nu}(\lambda')E_{\mu\nu} = \frac{1}{2}\left[\delta_{\lambda\lambda'} + \frac{\xi_3}{2}(\lambda\lambda' - 1) + i\frac{\xi_1}{2}(\lambda - \lambda') + \frac{\xi_2}{2}(\lambda + \lambda')\right] \qquad (2.5)$$

Photon $e^{\pm}$ cross-sections will be calculated with the usual normalization:

$$\sigma = (2\pi)^4 \frac{m_e}{s}\int d\rho_f \, |R_{fi}|^2 \qquad (2.6)$$

with the phase space

$$d\rho_f = \left(\prod \frac{N}{(2\pi)^3}\cdot\frac{d_3p}{p^0}\right)\delta_4(P_f - q)$$

and $N = m$ or $1/2$ for fermions or bosons.

For γe^- or γe^+ collisions we shall write the amplitude as $R_{fi} = \varepsilon^{\mu}\bar{t}_{\mu}u(\ell,\xi)$ or $R_{fi} = \varepsilon^{\mu}\bar{v}(\ell,\xi)t_{\mu}$; the polarization dependence of the cross-sections will appear through

$$|R_{fi}|^2 = E^{\mu\nu}\,Tr\left(\rho_e\, T_{\mu\nu}\right)$$

with $T_{\mu\nu} \equiv t_{\nu}\bar{t}_{\mu}$ or $t_{\mu}\bar{t}_{\nu}$ respectively.

The unpolarized case is obtained by putting P_L, P_T, $\bar{\lambda}$ and ζ_i to zero.

Neglecting $m_e/\sqrt{s}$ means that if no other massive lepton appears in the process and if no final polarization is measured, the initial $e^{\pm}$ transverse polarization P_T will not appear; only the longitudinal component P_L remains. The integrated cross-section of any process $\gamma e \to (f)$ giving a final state (f) will have the general form:

$$\sigma = \sigma_0 + \sigma_1 P_L + \sigma_2\bar{\lambda} + \sigma_3\bar{\lambda}P_L \qquad (2.7)$$

without $e^{\pm}$ transverse or γ linear polarization terms.

Differential cross-sections (for example two-body reactions $\gamma e \to A + B$) will in general have P_T and $\vec{\zeta}$ dependences associated with azimuthal terms ($\cos\phi$, $\sin\phi$, $\cos2\phi$, $\sin2\phi$).

For two-body reactions $\gamma e \to B + F$ where B and F represent bosonic and fermionic states, we shall use the kinematical invariants:

$$t=(k-B)^2=(\ell-F)^2, \quad u=(k-F)^2=(\ell-B)^2, \quad s+t+u \simeq m_B^2+m_F^2 .$$

In the γe centre-of-mass frame of Fig. 2, (θ,ϕ) being the angles of the direction of the fermion momentum $\vec{F}$, we have:

$$t = m_F^2 - 2\ell(F^0 - F\cos\theta) = m_B^2 - 2\ell(B^0 - B\cos\theta)$$
$$u = m_F^2 - 2\ell(F^0 + F\cos\theta) = m_B^2 - 2\ell(B^0 + B\cos\theta) .$$

It will be convenient to compare the magnitude of γe cross-sections with the point-like cross-section defined in e^+e^- annihilation[2] $\sigma_0 = 4\pi\alpha^2/3s$ and to use units of $R = \sigma/\sigma_0$. The simplest QED reaction in γe collisions, i.e., Compton scattering $\gamma e \to \gamma e$, as well as several other simple reactions, appear to have cross-sections with a magnitude of the order of $\sigma_0(R\simeq 1)$. In order to appreciate numbers given later on let us recall that

$$\sigma_0 \simeq \frac{87\ \text{nb}}{s(\text{GeV}^2)} , \quad \text{i.e. } \sigma_0 \simeq 35, 14, 9\ \text{pb for } \sqrt{s} = 50, 80, 100\ \text{GeV}$$

$(1\ \text{nb} = 10^3\ \text{pb} = 10^{-33}\ \text{cm}^2)$.

In Appendices A and B more technical details are given such as Dirac matrices, standard electroweak couplings and Lorentz transformations from the γe c.m. frame to other frames.

2b. Quasi-real $\gamma e^\pm$ collisions in e^+e^- inelastic scattering

The one-photon exchange process in e^+e^- inelastic scattering $[e'+e^\pm \to e'+(F^\pm)]$ indirectly allows $\gamma e^\pm$ to be reached, see Fig. 1. It will be interesting to compare the advantages and drawbacks of direct $\gamma e^\pm$ collisions at linear colliders with those of quasi-real $\gamma e^\pm$ collisions at conventional e^+e^- storage rings.

The e^+e^- inelastic process becomes important when at least one lepton (e') is scattered forwards; in this case the photon propagator is very large because $k^2 = (p-p')^2 = 2m_e^2 - 2p^0p'^0 + 2pp'\cos\theta$ almost vanishes. The final state $(F^\pm)$ of the $\gamma e^\pm$ collision propagates in the direction of the incident $e^\pm$ beam with a total momentum $|\vec{F}| = (E^2-s)/2E$, E being the total energy in the e^+e^- c.m. and $\sqrt{s}$ the invariant mass of the $\gamma e^\pm$ or $(F^\pm)$ system.

We write the amplitude corresponding to the process of Fig. 1 as:

$$R_{fi} = -\frac{eQ'}{k^2}\,\bar{u}(p')\,\gamma^{\mu}\,u(p)\,J_{\mu} \quad . \tag{2.8}$$

$\epsilon^{\mu}J_{\mu}$ would correspond to the subamplitude of the $\gamma e^{\pm}$ collision and Q' is the charge of the lepton e' which emits the photon. For each $\gamma e^{\pm} \to (F^{\pm})$ subprocess for which J_{μ} is known, one can calculate exactly the cross-section of $e'e^{\pm} \to e'F^{\pm}$:

$$\frac{p'^{0}d\sigma}{d_3 p'} = \frac{2\pi m_e}{E^2}\int d\rho_F\; L_{\mu\nu}\,J^{\mu}J^{\nu *} \tag{2.9}$$

with

$$L_{\mu\nu} = p_{\mu}p'_{\nu} + p_{\nu}p'_{\mu} - p\cdot p' g_{\mu\nu} + iQ'P'_L\,\varepsilon_{\mu\nu\rho\sigma}\,p^{\rho}p'^{\sigma} \tag{2.10}$$

P'_L being the longitudinal polarization of the incident lepton e'. In any case one can use the quasi-real approximation[2)-4)] for the estimation of the cross-section integrated over the polar angle θ of the scattered lepton; it consists of retaining only the components of J_{μ} transverse to k_{μ} and taking their values at $k^2 = 0$. The result can be written

$$\frac{d\sigma}{ds} = \left[\frac{(2E^2-s)^2+s^2}{s}\,\sigma_T - 2Q'P'_L(2E^2-s)\,\bar{\sigma}_T\right]\frac{\alpha}{4\pi}\,\mathrm{Log}\,\frac{E^2(E^2-s)^2}{m_e^2 s^2} \tag{2.11}$$

where

$$\sigma_T = \tfrac{1}{2}\left[\sigma(+) + \sigma(-)\right] \quad , \quad \bar{\sigma}_T = \tfrac{1}{2}\left[\sigma(+) - \sigma(-)\right]$$

are respectively $\gamma e^{\pm}$ cross-sections with unpolarized and circularly polarized quasi-real photons. See Section 5 for a similar application and more details about the quasi-real approximation. The linear photon polarization dependence disappeared during the integration over the azimuthal angle of the scattered lepton $e'(p')$. The circular photon polarization exists only when the incident lepton e' is itself longitudinally polarized.

In the simplest unpolarized case let us write:

$$\frac{d\sigma}{dz} = K(E,z)\,\sigma_T \tag{2.12}$$

with

$$K(E,z) = \frac{2\alpha}{\pi z}\left[\left(1-\frac{z^2}{2}\right)^2 + \frac{z^4}{4}\right]\mathrm{Log}\,\frac{E^2(1-z^2)^2}{m_e^2 z^4}$$

the quasi-real photon emission factor with $z = \sqrt{s}/E$. $K(E,z)$ is a rapidly decreasing function of z for E fixed. The same factor will be studied in Section 5 (see Fig. 14 and replace E^2 by s and z by x). For $E \simeq 100$ GeV and $z \simeq 1/2$, $K(E,z) \simeq 0.1$. This expression supposes no experimental angular cut-off, no strong k^2 dependence of the $\gamma e^{\pm}$ cross-sections and it neglects m_e everywhere except in the photon propagator.

In the case of a single fermion $F^{\pm}$ of mass M_F, spin $J = 1/2$ and partial decay width $\Gamma_{\gamma e}$ for $F^{\pm} \to \gamma e^{\pm}$ one can write:

$$\sigma\left(e'e^{\pm} \to e'F^{\pm}\right) = \frac{8\pi^2}{M_F^3}\,\Gamma_{e\gamma}\; z\, K(E,z) \qquad (2.13)$$

with $z = M_F/E$.

If one considers the particular case of $\gamma e^{\pm} \to (B) + e^{\pm}$ itself going through one photon exchange (see Section 5) the corresponding inelastic process $e^+e^- \to$ $\to e^+e^- + (B)$ goes through a double quasi-real photon exchange. Instead of applying the single photon emission factor $[K(E,z)K(s,x)]$ twice one can use directly the $\gamma\gamma$ luminosity factor in e^+e^- scattering[2)-4)]:

$$\frac{d\sigma}{dy}^{e^+e^- \to e^+e^-(B)} = K_{\gamma\gamma}(E,y)\;\sigma^{\gamma\gamma \to (B)} \qquad (2.14)$$

with

$$K_{\gamma\gamma}(E,y) = \frac{2}{y}\left[\left(1+\frac{y^2}{2}\right)^2 \log\frac{1}{y^2} - \frac{1}{2}\left(1-y^2\right)\left(3+y^2\right)\right]\left(\frac{\alpha}{\pi}\,\mathrm{Log}\,\frac{s}{m_e^2}\right)^2$$

for $y = W/E$, W being the $\gamma\gamma$ invariant mass. In the case of a single boson B of mass M, spin J and $\gamma\gamma$ decay width $\Gamma_{\gamma\gamma}$:

$$\sigma^{e^+e^- \to e^+e^- B} = \frac{4\pi^2(2J+1)\,\Gamma_{\gamma\gamma}}{M^3}\; y\, K_{\gamma\gamma}(E,y) \qquad (2.15)$$

with $y = M/E$.

For each $\gamma e^{\pm} \to (F^{\pm})$ reaction using the above approximation it is now easy to compare cross-sections of direct $\gamma e^{\pm}$ collisions with those of $e^+e^- \to e^{\mp} F^{\pm})$ going through quasi-real photon exchange. With a high energy storage ring (total c.m. energy $E = 100$ to 200 GeV) the obtainment of high energy $\gamma e^{\pm}$ collisions ($\sqrt{s} = 50$ to 100 GeV, i.e., $z \gtrsim 1/2$) costs a factor K less than 0.1. This may be compensated for by a higher initial luminosity. The designed e^+e^- luminosity is fixed between 10^{31} and 10^{32} cm^{-2} sec^{-1} [5)] for the storage ring projects, whereas for direct $\gamma e^{\pm}$ collisions at the SLC the luminosity was

estimated to be around 10^{30} cm^{-2} sec^{-1} [1]. On the other hand, the kinematics of direct $\gamma e^{\pm}$ collisions is simple. So it is only with a precise estimation of detection efficiencies and background problems that one will be able to conclude that one way is better than the other for each particular $\gamma e^{\pm} \to (F^{\pm})$ channel.

3. - QED REACTIONS

3a. Compton scattering

At lowest order in QED the reaction $\gamma e^{\pm} \to \gamma e^{\pm}$ is described by the two diagrams of Fig. 3. With the standard couplings[2] one gets the differential cross-section

$$\frac{d\sigma}{d\Omega} = \frac{\alpha^2}{2s}\left[\frac{t}{u}(1+\bar{\lambda}P_L) + \frac{t}{s}(1-\bar{\lambda}P_L) + 2\right] . \qquad (3.1)$$

There is no effect of $e^{\pm}$ transverse polarization or of γ linear polarization because $m_e \simeq 0$. The u and s poles can be killed by choosing longitudinal photon and electron polarizations $\bar{\lambda} = P_L$ or $\bar{\lambda} = -P_L$ respectively. The unpolarized cross-section[6]:

$$\frac{d\sigma}{d\Omega}^{NP} = \frac{\alpha^2}{2s}\left(\frac{t}{u} + \frac{t}{s} + 2\right) \qquad (3.2)$$

is strongly peaked backwards. This peak provides for the major part of the integrated cross-section. Keeping the electron mass term in the propagator $1/u-m_e^2$, one gets:

$$\sigma^{NP} = \frac{\pi\alpha^2}{s}\left[1 + 2\,\mathrm{Log}\left(1 + \frac{s}{m_e^2}\right)\right] . \qquad (3.3)$$

For example, at $\sqrt{s}$ = 100 GeV one gets $\sigma^{NP} \simeq 330$ pb (i.e., $R \simeq 36$); the large angle contribution $30^0 \leq \theta \leq 150^0$ is only $\sigma^{NP} \simeq 47$ pb (i.e., $R = 5.3$). This reaction provides tests of QED for fermionic channels. It is complementary to the crossed reaction $e^+e^- \to \gamma\gamma$ (with u and t channel electron exchanges). Here we have the new feature corresponding to electron formation with s large and time-like.

The discussion of QED violations done for $e^+e^- \to \gamma\gamma$ can be applied to $\gamma e \to \gamma e$ in a similar way. For example, one can look for modified electron exchange amplitudes, $ee\gamma\gamma$ seagull terms and excited electron (e^*) effects[7),8)].

3b. Intrinsic QED violations

Modifications of the electron exchange amplitude can be carried out provided that Ward identities and gauge invariance are satisfied. This has been studied for a long time now[7]. We give here the simplest application. Let us try to modify the s channel and u channel amplitudes of Fig. 3 by functions $F_s(s)$ and $F_u(u)$ respectively; gauge invariance requires the introduction of a seagull term (Fig. 4) and the complete amplitude is now:

$$R_{fi} = -e^2\, \bar{u}(\ell')\, \mathcal{O}\, u(\ell) \qquad R_{fi} = e^2\, \bar{v}(\ell)\, \mathcal{O}\, v(\ell')$$

(in the case of e^- and e^+ respectively)

with:

$$\mathcal{O} = \frac{\not\varepsilon'^{*} \not q \not\varepsilon}{s} F_s(s) + \frac{\not\varepsilon \not q' \not\varepsilon'^{*}}{u} F_u(u) + \frac{F_u(u) - F_s(s)}{t} \left[\varepsilon.\varepsilon'^{*} (\not k + \not k') - 2\varepsilon.k \not\varepsilon'^{*} - 2\varepsilon'^{*}.k \not\varepsilon \right] \tag{3.4}$$

$$q = \ell + k = \ell' + k' \quad , \quad q' = \ell' - k = \ell - k'$$

and

$$\frac{F_u(u) - F_s(s)}{t}$$

regular at $t = 0$. Functions $F_s(s)$ and $F_u(u)$ can be different for e^- and for e^+. The resulting cross-section is now:

$$\begin{aligned} \frac{d\sigma}{d\Omega} = \frac{\alpha^2}{2s} \Bigg\{ & |F_s(s)|^2 \left[-\frac{u(s^2+u^2)}{st^2} - \bar{\lambda} P_L \frac{u(u-s)}{st} \right] \\ & + |F_u(u)|^2 \left[\frac{2s^2}{t^2} - \frac{s}{u} - \bar{\lambda} P_L \frac{s(u-s)}{ut} \right] \\ & + 2\, \mathrm{Re}\, F_s(s) F_u^{*}(u) \left[\frac{2us}{t^2} - 1 + \bar{\lambda} P_L \left(1 + \frac{2s}{t} \right) \right] . \end{aligned} \tag{3.5}$$

A simple QED departure satisfying the preceding requirements can be described with a scalar parameter Λ:

$$\begin{aligned} F_s(s) &= 1 - b \frac{s}{\Lambda^2} + c \frac{s^2}{\Lambda^4} + \cdots \\ F_u(u) &= 1 + b \frac{u}{\Lambda^2} + c \frac{u^2}{\Lambda^4} + \cdots \end{aligned} \tag{3.6}$$

which gives:

$$\frac{d\sigma}{d\Omega} = \frac{d\sigma^{QED}}{d\Omega} - \frac{\alpha^2 c}{s\Lambda^4}\left[u^2+s^2+\bar{\lambda}P_L\, t(u-s)\right]+\cdots \qquad (3.7)$$

The violations do not appear at order $1/\Lambda^2$ [4]. In the case of $e^+e^- \to \gamma\gamma$ the present experimental status[9] is

$$\frac{|c|}{\Lambda^4} \lesssim \left(\frac{1}{50\,GeV}\right)^4 .$$

Notice that like $e^+e^- \to \gamma\gamma$ there is no weak effect expected to appear at second order in the $\gamma e \to \gamma e$ amplitude[10].

3c. Excited electron (e^*) effects

If such a state exists it can appear in exchange processes (u channel) and in formation processes (s channel) (Fig. 5). Let us write the gauge invariant γee^* coupling as:

$$L = \frac{e}{2}\bar{\psi}_{e^*}\sigma^{\mu\nu}(a-ib\gamma_5)\psi_e F_{\mu\nu} + h.c. \qquad (3.8)$$

This form generalizes the one first introduced by Low[11]. L will be charge conjugation invariant if a and b are real and will be CP invariant if a is real but b purely imaginary.

We have calculated the complete cross-section of $\gamma e^\pm \to \gamma e^\pm$ due to the four diagrams of Figs. 3 and 5 (square terms and interference terms). Its expression is given in Appendix C for the polarized case. The new features with respect to the QED part is the appearance of $e^\pm$ transverse polarization terms and of γ linear polarization terms associated with the e^* mass. Differences between γe^- and γe^+ cross-sections also appear with C violating terms odd in the b coupling constant and always associated with polarizations.

In the unpolarized case the differential cross-section has a simpler expression:

$$\frac{d\sigma^{NP}}{d\Omega} = \frac{\alpha^2}{2s}\left\{\frac{t}{u}+\frac{t}{s}+2+2\left(|a|^2+|b|^2\right)\left[\frac{s^2(s-M^2)}{(s-M)^2+M^2\Gamma^2}+\frac{u^2}{u-M^2}\right]\right. \qquad (3.9)$$

$$
\begin{aligned}
&- (|a|^2+|b|^2)^2 (su+tM^2)\left[\frac{s^2}{(s-M^2)^2+M^2\Gamma^2}+\frac{u^2}{(u-M^2)^2}\right] \\
&- 4(\mathrm{Im}\, ab^+)^2 (su-tM^2)\left[\frac{s^2}{(s-M^2)^2+M^2\Gamma^2}+\frac{u^2}{(u-M^2)^2}\right] \\
&- \frac{2M^2 stu\,(s-M^2)}{(u-M^2)\left[(s-M^2)^2+M^2\Gamma^2\right]}\left[(|a|^2+|b|^2)^2-4(\mathrm{Im}\, ab^+)^2\right]\Bigg\}
\end{aligned}
\qquad (3.9)\ \text{cont.}
$$

M and Γ being the mass and total width of the e^*. If M is much larger than the available energy ($M \gg \sqrt{s}$) the e^* effect will simply look like an intrinsic QED violation. The first-order correction term can be identified with Eq. (3.7) as:

$$
\frac{c}{\Lambda^4} = \frac{|a|^2+|b|^2}{M^2} \quad . \qquad (3.10)
$$

Notice that a and b are magnetic and electric dipole transitions with dimension M^{-1}. It is in this way that experimental limits are presently given[9] on the e^* effect in $e^+e^- \to \gamma\gamma$. They can be written as

$$
\frac{|a|^2+|b|^2}{M^2} \lesssim \left(\frac{1}{50\ \mathrm{GeV}}\right)^4 . \qquad (3.11)
$$

But the peculiar interest of γe scattering is the possibility of observing the e^* as a resonance if one can reach the energy $\sqrt{s} \simeq M$. In this case the cross-section is dominated by the Breit-Wigner form:

$$
\sigma \simeq \frac{8\pi}{s} \cdot \frac{(M\Gamma_{e\gamma})^2}{(s-M^2)^2+M^2\Gamma^2} \qquad (3.12)
$$

with the partial width of $e^* \to e\gamma$:

$$
\Gamma_{e\gamma} = \frac{\alpha M^3}{2}(|a|^2+|b|^2) . \qquad (3.13)
$$

For a narrow object the observation of the resonance peak will be possible if the energy resolution Δ is not too high. For $\Gamma < \Delta$ the integrated spectrum

$$
\overline{\sigma} = \int \sigma\, d\sqrt{s} = \frac{4\pi^2}{M^2}\Gamma_{e\gamma} \qquad (3.14)
$$

will be comparable to or larger than an $R = 1$ flat background if

$$
\Gamma_{e\gamma} \gtrsim \frac{M^2}{4\pi^2}\sigma_0 \Delta \qquad (3.15)
$$

i.e.,

$$\Gamma_{e\gamma} \gtrsim (5\,\mathrm{keV})\,\Delta$$

(Δ being expressed in GeV).

The e^* production could also be remarkable in e^+e^- inelastic scattering ($e^+e^- \to e^{\mp}e^{*\pm}$). A direct computation of the γ exchange process of Fig. 1 using the couplings (3.8) gives:

$$\frac{d\sigma}{d\Omega} = \frac{\alpha^2(S-M^2)}{ST}\Big\{\Big[|a|^2+|b|^2+2Q_e P_L \mathrm{Im}\,ab^+\Big]\big(2US+M^2(T-M^2)\big)$$
$$-Q'P_L'\Big[2Q_e \mathrm{Im}\,ab^+ + P_L(|a|^2+|b|^2)\Big]M^2(U-S)$$
$$+Q'P_L'P_T M\sqrt{S}(S-M^2)\sin\theta\Big[(|a|^2-|b|^2)\cos(\beta-\varphi)+2\,\mathrm{Re}\,ab^+\sin(\beta-\varphi)\Big]\Big\} \quad (3.16)$$

using notations of Section 2 and $S = 4E^2$, $T = (p-p')^2$, $U = (\ell-p')^2$.

This angular distribution of the scattered lepton $e'(p')$ is obviously strongly peaked forward because of the $1/T$ photon propagator. The integrated cross-section agrees with the quasi-real approximation given in Section 2b using $\Gamma_{e\gamma}$ given above:

$$\sigma^{e^+e^-\to e^{\pm}e^{*\mp}} = \frac{8\pi^2}{M^3}\Gamma_{e\gamma}\, z\, K(E,z) \quad (3.17)$$

with

$$z = \frac{M}{E}\,.$$

The observability (for $M < E$) is again controlled by the magnitude of $\Gamma_{e\gamma}$. For example, $\sigma(e^+e^- \to e^{\pm}e^{*\mp})$ will be larger than the point-like cross-section σ_0 if:

$$\Gamma_{e\gamma} \gtrsim \frac{M^3}{8\pi^2}\cdot\frac{\sigma_0}{z\,K(E,z)} \quad (3.18)$$

i.e.,

$$\Gamma_{e\gamma} \gtrsim (50\,\mathrm{keV})\,M$$

(M expressed in GeV).

This limit may appear less interesting than the corresponding one for direct $\gamma e^{\pm}$ collisions, but one should take into account other factors such as initial luminosities (see discussion at the end of Section 2b).

3d. High order processes

At third order in QED $\gamma e^{\pm}$ can do bremsstrahlung ($\gamma e \to \gamma\gamma e$) and pair production ($\gamma e \to L^+L^-e$); see Ref. 12) and standard books on QED. At higher orders one finds all possibilities of radiative corrections, purely electromagnetic ones like in $e^+e^- \to \gamma\gamma$ [13] as well as general electroweak radiative corrections with virtual Z, $W^{\pm}$ and Higgs boson effects[10].

At the present stage of this study we treat only the case of pair production. It may be especially interesting for monitoring the collisions, for γ polarization analysis as well as for the search for new lepton pairs. Pair production can appear through two kinds of processes - photon exchange and virtual Compton depicted in Figs. 6a and 6b (both of them are separately gauge invariant). Photon exchange processes are largely dominant and in the following we only discuss their contribution.

In the polarized case the expression of the cross-section is given in Appendix D. It can be useful for analyzing the initial photon linear polarization using e^+e^- or $\mu^+\mu^-$ pair production. In order to estimate the rates one now specifies the unpolarized case with a pure one-photon exchange. The totally differential cross-section of $\gamma e^{\pm} \to L^+L^-e^{\pm}$ is:

$$\frac{d\sigma}{dW^2 d\Omega d\Omega^*} = \frac{\alpha^3}{\pi s}\cdot\frac{\ell'}{\sqrt{s}}\cdot\frac{p^*}{W}\cdot\frac{1}{(k'^2)^2}\left\{\left[2\ell'.p'\ell.p'(3m^2-q'^2)+(\ell'.p\,\ell.p'+\ell'.p'\ell.p)(m^2-q'^2)-t.\ell'(4m^4+q'^2q'.p)\right]/(q'^2-m^2)^2\right.$$
$$+\left[p\leftrightarrow p'\right]$$
$$+2\left[-2\ell'.p\,\ell.p\,k'.p'-2\ell'.p'\ell.p'k'.p-(\ell'.p\,\ell.p'+\ell'.p'\ell.p)(2m^2+k.(p+p'))\right.$$
$$\left.\left.+\ell.\ell'(p.p'(2m^2+k'.(p+p'))+m^2k'.(p+p'))\right]/(q'^2-m^2)(q''^2-m^2)\right\} \quad (3.19)$$

where ℓ' is the final $e^{\pm}$ momentum with solid angle Ω in the $\gamma e^{\pm}$ c.m.; $\ell' = (s-W^2)/2\sqrt{s}$; $k' = \ell - \ell'$; p and p' are the momenta of L^- and L^+ with three-momentum p^* and solid angle Ω^* in the $\gamma\gamma$ or L^+L^- c.m.; $p^* = ((W^2/4)-m^2)^{1/2}$; W is the invariant mass of the L^+L^- pair; m is the $L^{\pm}$ mass.

Because of the photon propagator $1/k'^2$ the pair is mainly produced along the incident photon direction. In Section 5, Eq. (5.27), we shall give an approximate expression of the cross-section using the dominance of quasi-real photon exchange. The cross-section is a rapidly decreasing function of W. For a given lepton mass m, $d\sigma/dW^2$ peaks just above the threshold $W = 2m$. For very light fermions $(e^{\pm},\mu^{\pm})$ its magnitude is very high. For example, σ reaches several millibarns in the case of e^+e^- pairs. However, this is not very interesting except perhaps for monitoring, because their invariant mass is very low. For leptons with masses in the range of a few GeV the cross-section is of the order of the nanobarn, and for $m \simeq 20$ GeV it is still of the order of 10pb for $\sqrt{s} \simeq 100$ GeV (see Section 5c and Fig. 19 for more details). All these features are similar to those of pair production by $\gamma\gamma$ collisions in $e^+e^- \to e^+e^-L^+L^-$ processes. Again the cross-sections of direct $\gamma e^{\pm}$ collisions are larger by an order of magnitude, but one should take into account initial luminosities and background problems. The search for heavy leptons in $\gamma\gamma$ collisions has been particularly discussed in the high energy storage ring project reports[5].

4. - Z^0 and $W^{\pm}$ PRODUCTION

4a. $\gamma e \to Ze$

This reaction is similar to Compton scattering except for the occurrence of vector and axial couplings at Zee vertices and for Z mass effects. With the two diagrams of Fig. 7 one gets the differential cross-section:

$$\frac{d\sigma}{d\Omega} = \frac{\alpha^2 p}{s\sqrt{s}} \left\{ \left[a^2+b^2+2ab\,Q_e P_L\right]\left[2 - \frac{(t-M_Z^2)^2}{su} - \frac{2M_Z^2 p^2 \sin^2\theta}{u^2}\left(1+\xi_3\cos 2\varphi - \xi_1 \sin 2\varphi\right)\right] \right.$$
$$\left. + \bar{\lambda}\left[P_L(a^2+b^2)+2ab\,Q_e\right]\frac{(t+M_Z^2)(s-u)}{su} \right\} \qquad (4.1)$$

where $p = (s-M_Z^2)/2\sqrt{s}$ and a and b are the Zee coupling constants whose values in the standard case are given in Table 1.

As compared to Compton scattering (obtained with $a = -1$, $b = 0$, $M_Z = 0$) one observes γ linear polarization effects with azimuthal $\cos 2\phi$ and $\sin 2\phi$ dependences associated with Z mass terms. Electron and positron cases differ also by C violating terms linear in the axial coupling b. The angular

distribution is again strongly peaked backwards, see Fig. 8. This is due to the dominance of the u channel diagram which can be viewed as an almost real $e^+e^- \to Z$ annihilation after the $\gamma \to e^+e^-$ pair creation. At high energy the Z decay products will be found along the incident $e^\pm$ direction. In the unpolarized case the integrated cross-section is given by:

$$\sigma^{NP} = \frac{\pi\alpha^2(a^2+b^2)}{s}\left\{1+6\frac{M_Z^2}{s}-7\left(\frac{M_Z^2}{s}\right)^2+2\left[1-2\frac{M_Z^2}{s}+2\left(\frac{M_Z^2}{s}\right)^2\right]\mathrm{Log}\frac{(s-M_Z^2)^2}{m_e^2(2s-M_Z^2)}\right\} . \quad (4.2)$$

It gets its maximum just above the threshold ($\sqrt{s} \simeq M_Z + 2.5$ GeV) with a value of 0.09 nb. At higher energies it reaches $(|a|^2 + |b|^2)$ times the Compton cross-section (see Fig. 9), i.e., a factor 0.38 if one uses $\sin^2\theta_W \simeq 0.215$. This corresponds to $R \simeq 8$ between $\sqrt{s} \simeq 100$ GeV and 150 GeV.

For Z^0 production this reaction should not be competitive with direct e^+e^- annihilation. It nevertheless gives independent tests of Z^0 couplings and Z^0 structure. For example, it can check (as in $e^+e^- \to \gamma Z$ [14]) the absence of anomalous $\gamma\gamma Z$ or γZZ couplings which would occur in (γ,Z) exchange diagrams in the t channel.

4b. $\gamma e \to W\nu_e$

$W^\pm$ production proceeds via the two diagrams of Fig. 10. With the Yang-Mills γWW and the V-A $We\nu_e$ couplings [see Appendix A and Ref. 2)] the resulting cross-section is:

$$\frac{d\sigma}{d\Omega} = \frac{\alpha^2}{8s\sin^2\theta_W}(1+Q_eP_L)\frac{p}{\sqrt{s}}\left\{(1+Q_e\bar{\lambda})\left[2\left(1-\frac{M_W^2}{s}\right)+\frac{t}{s}\left(2-\frac{s}{M_W^2}\right)\right]\right.$$
$$+\frac{2}{(t-M_W^2)^2}\left[-2us-\frac{t}{2}(1+Q_e\bar{\lambda})\frac{(t-M_W^2)^2}{M_W^2}-2tp^2\sin^2\theta\,(1+\Sigma_3\cos 2\varphi-\Sigma_1\sin 2\varphi)\right] \quad (4.3)$$
$$-\frac{2}{s(t-M_W^2)}\left[(1+Q_e\bar{\lambda})\left(2su+st\left(1-\frac{t}{M_W^2}\right)+Q_e\bar{\lambda}\left(t(M_W^2-t)+s(s-M_W^2)+u(M_W^2-u)\right)\right)\right.$$
$$\left.\left.-2sp^2\sin^2\theta\,(1+\Sigma_3\cos 2\varphi-\Sigma_1\sin 2\varphi)\right]\right\} .$$

The factor $(1+Q_eP_L)$ reflects the V-A structure of $We\nu_e$ couplings; the cross-section vanishes for right-handed electrons or left-handed positrons. Further

$Q_e\lambda$ factors reflect the C violating axial terms. There are also γ linear polarization dependences coming from the γWW coupling and the W exchange diagram. We have here interesting possibilities of testing the Yang-Mills form of γWW couplings.

At moderate energies the reaction $\gamma e \to W\nu$ has a behaviour somewhat different from the $\gamma e \to Ze$ one because both W and electron exchanges are far from mass-shell. The angular distribution of $\gamma e \to W\nu$ is slightly peaked forward due to $1/t-M_W^2$ terms as shown in Fig. 11. The integrated cross-section is also weaker than the one of $\gamma e \to Ze$. In the unpolarized case it can be written[1)15)]

$$\sigma^{NP} = \alpha G\sqrt{2}\left[1+\frac{1}{4}\left(\frac{M_W^2}{s}\right)+\frac{1}{2}\left(\frac{M_W^2}{s}\right)^2-\frac{7}{4}\left(\frac{M_W^2}{s}\right)^3+\frac{M_W^2}{s}\left(2+\frac{M_W^2}{s}+\left(\frac{M_W^2}{s}\right)^2\right)\log\frac{M_W^2}{s}\right] \qquad (4.4)$$

using $$G\sqrt{2} = \frac{e^2}{4M_W^2\sin^2\theta_W} .$$

One gets $\sigma \simeq 1.7$ pb for $\sqrt{s} \simeq 100$ GeV and 8 pb for $\sqrt{s} \simeq 140$ GeV. It is only at very high energies ($\sqrt{s} >> M_W$) that the W exchange diagram strongly dominates and leads to an asymptotic constant value of 44 pb (see Fig. 12).

This may nevertheless be an interesting way of producing single $W^\pm$ bosons and testing γWW Yang-Mills couplings with energies less than those required for pair production in $e^+e^- \to W^+W^-$ ($\sqrt{s} > 2M_W$). The case of single $W^\pm$ production in inelastic e^+e^- scattering $e^+e^- \to e^\mp \nu W^\pm$ had already been studied for high energy storage ring projects[5),16)]. An exact calculation can be found in Ref. 17) with a cross-section appearing to be about 30 times lower than the present one for $\gamma e \to W\nu$. Questions of initial luminosities and backgrounds will be important particularly for such small cross-sections.

5. - BOSON EXCHANGE PROCESSES

5a. Generalities

In $\gamma e^\pm$ collisions there is a large class of interesting processes going through one boson exchange ($b \equiv \gamma$, Z or $W^\pm$). When $b \equiv \gamma$ they can be expressed in terms of the so-called $\gamma\gamma$ collision processes. These have been studied in detail for e^+e^- inelastic scattering $e^+e^- \to e^+e^- + (B)$ especially in the double quasi-real photon limit[2)-4)]. In the case of direct $\gamma e^\pm$

collisions one can reach real γ quasi-real γ collisions. This is the main aim of this section although we treat γZ and $\gamma W^{\pm}$ on the same footing (Fig. 13).

A rough comparison of orders of magnitude in e^+e^- inelastic scattering and in direct $\gamma e^{\pm}$ collisions can be made using the γ emission factors given in Section 2b. For the case of pure γ exchange in $\gamma e^{\pm}$ collisions the comparison can be made using the $\gamma\gamma$ luminosity factor $K_{\gamma\gamma}$ of Eq. (2.14) for e^+e^- scattering.

We restrict this study to the cases $\gamma e \to (B) + (F)$ whose (F) is a single fermion (e or ν_e). The more general cases with inelastic $e \to (F)$ transitions could also be considered.

The final fermion distribution has the general form:

$$\frac{\ell'^0 d\sigma}{d_3\ell'} = \frac{\pi e^2}{s\,|D(k')|^2}\, E^{\mu\nu}\, M_{\mu\nu\tau\tau'}\, L^{\tau\tau'} \tag{5.1}$$

where $E^{\mu\nu} = \varepsilon^{\mu}\varepsilon^{\nu *}$ (with its expression given in Section 2).

$$L^{\tau\tau'} = \left[|a|^2+|b|^2+2Q_e P_L \mathrm{Re}\, ab^*\right]\left(\ell'^{\tau}\ell^{\tau'} + \ell'^{\tau'}\ell^{\tau} - \ell.\ell' g^{\tau\tau'}\right) \tag{5.2}$$

$$-i\left[P_L(|a|^2+|b|^2) + 2Q_e \mathrm{Re}\, ab^*\right]\varepsilon^{\tau\tau'\rho\sigma}\ell_\rho \ell'_\sigma$$

is the leptonic tensor due to the ebF vertex using the couplings

$$L = -e\,\bar{\psi}_F\,\gamma^{\mu}(a-b\gamma^5)\,\psi_e\,\phi_{\mu} + h.c. \tag{5.3}$$

with standard coefficients a and b given in Table 1.

Notice that there is no transverse $e^{\pm}$ polarization dependence because we neglect m_e and m_F and we sum over final F spin states.

$$M_{\mu\nu\tau\tau'} = \int d\rho_B\; T_{\mu\tau}\, T^*_{\nu\tau'}$$

represents the γb collision process whose amplitude is $\varepsilon^{\mu}e^{\tau}T_{\mu\tau}$; $d\rho_B$ is the phase space of final state (B). $D(k')$ is the virtual boson propagator (k'^2 for $b = \gamma$, $k'^2 - m^2$ for $b = Z$ or $W^{\pm}$). We shall sometimes use helicity states in the γb c.m. frame, λ for the incident photon and η for the virtual boson b (see Appendix B for γb c.m. variables). In this case one can write

$$\frac{\ell'^0 d\sigma}{d_3\ell'} = \frac{2e^2 k^* W}{s(2\pi)^3 |D(k')|^2} \sum_{\lambda\lambda' bb'} E(\lambda\lambda')\,\sigma(\lambda\lambda' bb')\,L(bb') \tag{5.4}$$

or

$$\frac{d\sigma}{dW^2 d\Omega} = \frac{e^2 k^* W \ell'}{s\sqrt{s}(2\pi)^3 |D(k')|^2} \sum_{\lambda\lambda' bb'} E(\lambda\lambda')\,\sigma(\lambda\lambda' bb')\,L(bb') \tag{5.5}$$

Ω is the solid angle of the direction of the final fermion momentum $\vec{\ell}'$ in the γe c.m.; W and k^* are the invariant mass and the photon momentum in the γb c.m. $E(\lambda\lambda')$ is given by Eq. (B.1) of Appendix B; $L(\eta\eta') = N_\eta N_{\eta'} e^{\tau *}(\eta) e^{\tau'}(\eta') L_{\tau\tau'}$ is given in Eq. (B.2) and Table 2

$$\sigma(\lambda\lambda' bb') = \frac{(2\pi)^4}{4k^* W} M(\lambda\lambda' bb')$$

with

$$M(\lambda\lambda' bb') = \varepsilon^{\mu}(\lambda)\varepsilon^{\nu *}(\lambda') e^{\tau}(b) e^{\tau' *}(b') M_{\mu\nu\tau\tau'}$$

will be called the γb collision correlation. Its diagonal part ($\lambda = \lambda'$, $\eta = \eta'$) is exactly the polarized $\gamma b \to (B)$ cross-section $\sigma(\lambda\eta)$.

In the case of a single bosonic particle (B) of spin J and mass M one can use the $B \to \gamma b$ decay correlation:

$$\gamma(\lambda\lambda' bb') = \frac{k^*}{8\pi M^2 (2J+1)} \varepsilon^{\mu}(\lambda)\varepsilon^{\nu *}(\lambda') e^{\tau}(b) e^{\tau' *}(b') T_{\mu\tau} T^*_{\nu\tau'} \tag{5.6}$$

and write the angular distribution of $\gamma e \to BF$ as:

$$\frac{d\sigma}{d\Omega} = \frac{(2J+1) e^2 M^2 \ell'}{2\pi k^* s\sqrt{s}\,|D(k')|^2} \sum_{\lambda\lambda' bb'} E(\lambda\lambda')\,\gamma(\lambda\lambda' bb')\,L(bb') \ . \tag{5.7}$$

The diagonal part of the decay correlation averaged over angles coincides with the polarized partial decay width of $B \to \gamma b$:

$$\Gamma(\lambda b) = \frac{1}{4\pi} \int d\Omega^*\, \gamma(\lambda\lambda bb) \ .$$

Single γ exchange:

With the couplings $a = -1$, $b = 0$, the leptonic tensor is independent of the $e^{\pm}$ charge but still depends on the longitudinal $e^{\pm}$ polarization P_L. Parity invariance of the $\gamma\gamma(B)$ amplitude will constrain the form of the correlation:

$$M(\lambda\lambda' bb') = M(-\lambda-\lambda'-b-b') \ .$$

γ and Z exchange:

With Z exchange we have a and b couplings given by Table 1 for the standard model. Parity violation can also appear in the γZ(B) amplitudes.

If one wants to take into account both γ and Z exchange terms and their interference one has just to replace in Eqs. (5.4) and (5.5) the product

$$\frac{\sigma(\lambda\lambda' bb')\, L(bb')}{|D(k')|^2}$$

by

$$\sum_{\alpha,\beta} \frac{\sigma^{\alpha\beta}(\lambda\lambda' bb')\, L^{\alpha\beta}(bb')}{D_\alpha(k')\, D_\beta^*(k')}$$

where α and β both run over γ and Z (for example $L^{\alpha\beta}$ comes from a^α and b^α coupling constants).

$W^\pm$ exchange

In this case the final state F is ν_e or $\overline{\nu_e}$; the V-A structure of the $We\nu_e$ vertex gives simply:

$$|a|^2+|b|^2+2Q_e P_L \mathrm{Re}\, ab^* = 2\,\mathrm{Re}\, ab^* + Q_e P_L (|a|^2+|b|^2) = \frac{1+Q_e P_L}{4\sin^2\theta_W} \quad .$$

Obviously the reaction proceeds only for e^-_{left} or e^+_{right} polarization states. This fact can be used for background suppression.

Quasi-real γγ scattering:

In the case of single γ exchange one can use the dominance of the $k'^2 \simeq 0$ region (forward $e^\pm$ scattering) in order to approximate Eq. (5.5) by the contribution of quasi-real exchanged photons only. We keep only η, η' = ±1 helicities and take the collision amplitudes at $k'^2 = 0$. We neglect m_e^2 factors everywhere except in the expression of $D(k') = k'^2$. Integrating $L(\eta\eta')/|D(k')|^2$ over dΩ and using parity invariance for $\sigma(\lambda\lambda'\eta\eta')$ one gets the leading log result, with $x = W/\sqrt{s}$:

$$\frac{d\sigma}{dx} = \left[\left(1-x^2+\frac{x^4}{2}\right)\sigma_T(W) - Q_e\bar{\lambda} P_L (2-x^2)\frac{x^2}{2}\overline{\sigma_T}(W)\right]\frac{2\alpha}{\pi x}\,\mathrm{Log}\,\frac{s(1-x^2)^2}{m_e^2 x^4} \qquad (5.8)$$

where

$$\sigma_T(W) \equiv \tfrac{1}{2}\left[\sigma(++++)+\sigma(++--)\right] \equiv \tfrac{1}{2}(\sigma^0+\sigma^2)$$

$$\overline{\sigma_T}(W) \equiv \tfrac{1}{2}\left[\sigma(++++)-\sigma(++--)\right] \equiv \tfrac{1}{2}(\sigma^0-\sigma^2)$$

are purely transverse $\gamma\gamma \to (B)$ cross-sections taken at $k'^2 = 0$. $\sigma_T(W)$ is the spin averaged $\gamma\gamma$ cross-section, $\bar{\sigma}_T(W)$ is the difference of $\gamma\gamma$ cross-sections with total helicity $\lambda - \eta = 0$ and $\lambda - \eta = 2$. This last quantity is associated with longitudinal $e^{\pm}$ and circular γ polarizations.

The log term is the result of the approximation which consists of neglecting terms proportional to m_e^2, k'^2 dependence in the $\gamma\gamma$ cross-sections and experimental angular cut-offs. Notice also that linear photon polarization dependence has disappeared in the azimuthal integration. In the unpolarized case we can write:

$$\frac{d\sigma}{dx} = K(s,x)\ \sigma_T(W) \tag{5.9}$$

with

$$K(s,x) = \frac{2\alpha}{\pi x}\left(1 - x^2 + \frac{x^4}{2}\right) \log \frac{s(1-x^2)^2}{m_e^2 x^4}$$

the quasi-real emission factor that we can also call the $\gamma\gamma$ luminosity factor in direct γe collisions. It is a rapidly decreasing function of x for s fixed as shown in Fig. 14.

In the case of a single bosonic particle B^0 of mass M and spin J we can use the $\gamma\gamma$ decay widths:

$$\Gamma_{\gamma\gamma} = \frac{1}{2} \int \frac{d\Omega^*}{4\pi} \sum_{\lambda,\lambda'=\pm 1} \gamma(\lambda\lambda\lambda'\lambda')$$

(the factor 1/2 being introduced because of Bose statistics for real photons) and

$$\overline{\Gamma}_{\gamma\gamma} = \frac{1}{2}\left[\gamma(++++) - \gamma(++--)\right] \equiv \frac{1}{2}\left[\Gamma^0_{\gamma\gamma} - \Gamma^2_{\gamma\gamma}\right] .$$

We get the integrated cross-section for $\gamma e \to B^0 e$:

$$\sigma = \frac{8\pi\alpha(2J+1)}{M^3}\left[\left(1 - x^2 + \frac{x^4}{2}\right)\Gamma_{\gamma\gamma} - Q_e \bar{\lambda} P_L (2 - x^2) x^2 \overline{\Gamma}_{\gamma\gamma}\right] \log \frac{s(1-x^2)^2}{m_e^2 x^4} \tag{5.10}$$

with $x = M/\sqrt{s}$. In the unpolarized case it reduces to:

$$\sigma = 4\pi^2(2J+1)\ \frac{\Gamma_{\gamma\gamma}}{M^3} \times K(s,x) \quad . \tag{5.11}$$

Equations (5.9) and (5.11) can be used for the estimation of the cross-sections in terms of any particular $\gamma\gamma$ collision process, for example those already studied for $e^+e^- \to e^+e^- + (B)$ processes[2)-4)].

In direct $\gamma e^{\pm}$ collisions the level of the cross-sections seems interesting. For example, in the case of a single particle with a decay width $\Gamma_{\gamma\gamma}$ of the order of 1 keV the cross-section is appreciable up to very high mass values. For $\sqrt{s} \simeq 50$ to 100 GeV and M in the range of a few GeV:

$$\sigma \simeq (3\ \text{nb})\,(2J+1)\,\frac{\Gamma_{\gamma\gamma}(\text{keV})}{M^3_{(\text{GeV})}} \qquad (5.12)$$

There are several kinds of $C = +1$ states that one begins to observe in $\gamma\gamma$ processes or that one would like to observe[18)]: $q\bar{q}$ resonant states $(\varepsilon, f^0, A_2^0, \ldots)$, heavy quark states $(\eta_c, \chi_c, \ldots, \eta_b, \chi_b, \ldots)$, exotic states like glueballs or multi-quark states, elementary bosons, etc. In Table 3 we give a few examples of expected cross-sections in direct $\gamma e^{\pm}$ collisions. Again these cross-sections appear one order of magnitude larger than the ones of $\sigma(e^+e^- \to e^+e^-B)$. For M in the range of a few GeV and σ of several nanobarns there will surely be no special problems of detection. For very high mass states and cross-sections of the order of picobarns, questions of luminosities and backgrounds will again become important.

In the following subsections we give more details about the distributions of single bosons and of boson and fermion pairs produced by one-boson exchange

5b. Examples of single boson production

Spin zero boson:

We consider the case where B is a scalar or a pseudoscalar particle (Fig.15). In the general case (without parity conservation) we have the γbB couplings:

$$e^2\left[ig\,\varepsilon^{\mu\nu\rho\sigma}\varepsilon_\mu k_\nu e_\rho k'_\sigma + g'(\varepsilon.e\,k.k' - \varepsilon.k'\,e.k)\right]. \qquad (5.13)$$

They apply to the neutral $(b=\gamma,Z)$ as well as to the charge case $(b=W^{\pm})$. In the case of photon exchange with parity conservation the g coupling occurs for pseudoscalar production $(B=\pi^0,\eta,\eta_c,\ldots)$ and the g' coupling occurs for scalar production $(B=\varepsilon,\delta^0,\chi_c^0,\ldots)$. A direct computation gives the cross-section in the polarized case:

$$\frac{d\sigma}{d\Omega} = \frac{\pi\alpha^3 \ell'}{s\sqrt{s}\,|D(k')|^2} \Big\{ \big[|a|^2+|b|^2+2Q_e P_L \mathrm{Re}\, ab^*\big]\Big[|g|^2\Big(\tfrac{t}{2}(2su-(m_B^2-t)^2)-s^2\ell'^2\sin^2\theta(\xi_3\cos 2\varphi-\xi_1\sin 2\varphi)\Big)$$
$$+|g'|^2\Big(\tfrac{t}{2}(2su-(m_B^2-t)^2)+s^2\ell'^2\sin^2\theta(\xi_3\cos 2\varphi-\xi_1\sin 2\varphi)\Big)$$
$$-\bar\lambda t\,\mathrm{Re}\, g g'^*(s^2+u^2)+2\,\mathrm{Im}\, g g'^* s^2\ell'^2\sin^2\theta(\xi_3\sin 2\varphi+\xi_1\cos 2\varphi)\Big]$$
$$+\bar\lambda\Big[P_L(|a|^2+|b|^2)+2Q_e\,\mathrm{Re}\, ab^*\Big]\Big[\tfrac{t}{2}(m_B^2-t)(u-s)(|g|^2+|g'|^2)$$
$$+2\,\mathrm{Re}\, g g'^*(u-s)t(m_B^2-t)\Big]\Big\} \qquad (5.14)$$

For pure γ exchange this formula simplifies to:

$$\frac{d\sigma}{d\Omega} = \frac{\pi\alpha^3\ell'}{s\sqrt{s}\,t^2}|g|^2\Big\{stu-\tfrac{t}{2}(m_B^2-t)^2-s^2\ell'^2\sin^2\theta(\xi_3\cos 2\varphi-\xi_1\sin 2\varphi)+\bar\lambda P_L\tfrac{t}{2}(u-s)(m_B^2-t)\Big\} \qquad (5.15)$$

(for pseudoscalar production $\gamma e \to Pe$) and

$$\frac{d\sigma}{d\Omega} = \frac{\pi\alpha^3\ell'}{s\sqrt{s}\,t^2}|g'|^2\Big\{stu-\tfrac{t}{2}(m_B^2-t)^2+s^2\ell'^2\sin^2\theta(\xi_3\cos 2\varphi-\xi_1\sin 2\varphi)+\bar\lambda P_L\tfrac{t}{2}(u-s)(m_B^2-t)\Big\} \qquad (5.16)$$

(for scalar production $\gamma e \to Se$).

The unpolarized cross-sections have the same expressions in the case of P or S (one has just to replace g by g'). The integrated cross-sections agree with the quasi-real approximation and Eq. (5.11) using the partial widths:

$$\Gamma_{B\to\gamma\gamma} = \frac{\pi\alpha^2}{4} m_B^3 \left(|g|^2 \text{ or } |g'|^2\right). \qquad (5.17)$$

The only difference between P and S production is the sign of the γ linear polarization term which reflects the change of intrinsic parity.

In the case of pure Z or $W^{\pm}$ exchanges the magnitude of the cross-sections corresponds typically to a ratio

$$R \simeq (|a|^2+|b|^2)\,|\bar g|^2$$

where $\bar g$ is a dimensionless coupling constant which depends on mass ratios. For heavy bosons B one can expect to have $R \simeq 1$, i.e., cross-sections of the order of a few picobarns for $\sqrt{s} \simeq 100$ GeV. For the separation of such weak channels from

the background it may be especially interesting to use polarized beams and to construct longitudinal polarization asymmetries or $\gamma e^+ - \gamma e^-$ asymmetries which vanish in the case of pure electromagnetic interactions.

Spin one boson

B being a vector or axial particle there are in general four γbB couplings. The vertex is written

$$e^2 \sum_{i=1,4} g_i I_i$$

with

$$I_1 = ie.k\ \varepsilon^{\mu\nu\rho\sigma} k'_\mu k_\nu \varepsilon_\rho V^*_\sigma \qquad I_2 = iV^*.k'\varepsilon^{\mu\nu\rho\sigma} k'_\mu k_\nu \varepsilon_\rho e_\sigma$$
$$I_3 = \varepsilon.e\, V^*.k - \varepsilon.V^* e.k \qquad I_4 = e.k\,(\varepsilon.V^* k.B - \varepsilon.B\, V^*.k) \tag{5.18}$$

B^μ and V^μ being the four-momentum and the polarization of the spin one boson. In general, the cross-section can be computed using Eq. (5.7), Table 2 and the correlation:

$$\begin{aligned}\gamma(\lambda\lambda' bb') = \frac{k^*}{24\pi m_B^2}\Big\{ &-\frac{|g_1|^2}{t}(k^* m_B)^4 \delta_{\lambda\lambda'}\delta_{b0}\delta_{b'0} + |g_2|^2 k^{*4} m_B^2 \lambda\lambda' \delta_{\lambda b}\delta_{\lambda' b'} \\ &+ |g_3|^2 k^{*2}\Big(\delta_{\lambda b}\delta_{\lambda' b'} - \frac{m_B^2}{t}\delta_{\lambda\lambda'}\delta_{b0}\delta_{b'0}\Big) - |g_4|^2\Big(\frac{m_B^2 - t}{2}\Big)^2 \frac{k^{*2} m_B^2}{t}\delta_{\lambda\lambda'}\delta_{b0}\delta_{b'0} \\ &+ \mathrm{Re}\, g_1 g_3^* \frac{k^{*3} m_B^3}{t}(\lambda+\lambda')\delta_{b0}\delta_{b'0} - \mathrm{Re}\, g_1 g_4^* \frac{k^{*3} m_B^3}{t}\Big(\frac{m_B^2 - t}{2}\Big)(\lambda+\lambda')\delta_{b0}\delta_{b'0} \\ &- k^{*3} m_B \delta_{\lambda b}\delta_{\lambda' b'}\big[(\lambda+\lambda')\mathrm{Re}\, g_2 g_3^* + i(\lambda-\lambda')\mathrm{Im}\, g_2 g_3^*\big] + \mathrm{Re}\, g_3 g_4^* (m_B^2 - t)\frac{k^{*2} m_B^2}{t}\delta_{\lambda\lambda'}\delta_{b0}\delta_{b'0}\Big\}\end{aligned} \tag{5.19}$$

for $\lambda, \lambda' = \pm 1$ and $b, b' = \pm 1, 0$.

It applies directly to $W^\pm$ exchange in processes such as $\gamma e^\pm \to V^\pm \nu_e$ and $\gamma e^\pm \to A^\pm \nu_e$ with $V^\pm = \rho^\pm, K^\pm, D^{*\pm}, \ldots$ and $A^\pm = A_1^\pm, K_A^{*\pm}, \ldots$. [The case $\gamma e \to W^\pm \nu_e$ requires the gauge invariance constraint with the Compton-like diagram and has been calculated in Section 4b.] Notice that photon linear polarization appears only with $\mathrm{Im} g_2 g_3^*$ [use $E(\lambda\lambda')$ given by Eq. (B.1)].

In the case of Z exchange with first class (CP=+1) electroweak currents and $C_\gamma = -1$ only I_1 and I_2 couplings are allowed, so only the first two terms of $\gamma(\lambda\lambda'\eta\eta')$ remain. They control the reactions $\gamma e \to V^0 e$, $\gamma e \to A^0 e$ (V^0 and A^0 being elementary or bound vector and axial states) and eventually $\gamma e \to Ze$ if anomalous $ZZ\gamma$ couplings exist[14].

In the case of γ exchange with parity conservation only $\gamma e \to A^0 e$ (and eventually $\gamma e \to Ze$) is allowed for virtual $(t=k'^2 \neq 0)\gamma$ exchange. The contribution vanishes in the quasi-real limit (because of Bose statistics), so one loses the benefit of the $\log s/m_e^2$ factor and the cross-section becomes smaller by one order of magnitude.

5c. Pair production

Photon exchange processes (and Z, $W^\pm$ exchanges at a weaker level) are an interesting source of pair production (Bethe-Heitler[12]). Any kind of charged particle pair can be produced (spin zero, spin one, charged fermions, leptons, quarks,...). In general, the reaction proceeds via boson exchange processes and boson production processes (Compton-like) which can interfer (see Figs. 6a and 6b). The photon exchange process is largely the dominant one when the quasi-real limit is allowed. In this case the pair is produced along the incident photon direction. In this sub-section we treat only this class of process going through boson exchange. The cross-section of any of these boson exchanges can easily be computed using Eqs. (5.1) - (5.5), the phase space $d\rho_B$ of the pair and the amplitudes $T_{\mu\tau}$ of $\gamma b \to p^+p^-$. We now illustrate the charged spin zero and the fermion cases.

Charged spin zero pair: $\gamma e^\pm \to B^+B^-e^\pm$

The subprocess $\gamma b^0 \to B^+B^-$ is controlled by the three diagrams of Fig. 16 whose amplitude is

$$T^{\mu\tau} = -2e^2 g \left[\frac{p^\mu p'^\tau}{p.k} + \frac{p'^\mu p^\tau}{p'.k} - g^{\mu\tau} \right] . \qquad (5.20)$$

For $b^0 \equiv \gamma$ the quantity g is equal to $Q_B^2 = 1$ the square charge of $B^\pm$ in units of e. g would have different values for $b^0 \equiv Z^0$ depending on the model and the nature of the particles. On the helicity basis we can compute $F(\lambda\eta) = \varepsilon^\mu(\lambda)\, e^\tau(\eta)\, T_{\mu\tau}$:

$$F(\lambda b) = e^2 g \left\{ \lambda b\, p^{*2} \sin^2\theta^* e^{i(\lambda - b)p^*} \left[\frac{1}{p.k} + \frac{1}{p'.k} \right] + 2\,\delta_{\lambda b} \right.$$
$$\left. + \frac{\sqrt{2}\lambda}{\sqrt{-t}}\,\delta_{b0}\, p^* \sin\theta^*\, e^{-i\lambda p^*} \left[\frac{p'^{0*}k'^{*} + p'^{*}k'^{0*}\cos\theta^*}{p.k} - \frac{p^{0*}k'^{*} - p^{*}k'^{0*}\cos\theta^*}{p'.k} \right] \right\} \tag{5.21}$$

(all variables are here γb^0 c.m. variables).

The general form of the cross-section can then be obtained using Table 2, Eqs. (5.4) and (5.5) and $M(\lambda\lambda'\eta\eta') = 1/4(2\pi)^6 \cdot (p^*/W)\int d\Omega^* F(\lambda\eta)F^*(\lambda'\eta')$. In the case of unpolarized photons the result is simply:

$$\frac{d\sigma}{dW^2 d\Omega\, d\Omega^*} = \frac{\alpha^3 g^2 p^* \ell'}{4\pi^2 s W \sqrt{s}\, |D(k')|^2} \left[|a|^2 + |b|^2 + 2 Q_e P_L \mathrm{Re}\, a b^* \right] \cdot$$
$$\cdot \left\{ 2\ell\ell' - m^2 \left[\frac{2\ell.p'\ell'.p' - m^2 \ell.\ell'}{(p.k)^2} + \frac{2\ell.p\,\ell'.p - m^2\ell.\ell'}{(p'.k)^2} \right] + 2\left(\ell.p\ell'.p' + \ell'.p\ell.p' - \ell.\ell'\, p.p'\right) \frac{k.(p+p') - p.p'}{p.k\, p'.k} \right\}. \tag{5.22}$$

(It still applies to γ or Z^0 exchange.)

In the case of quasi-real γ dominance we can use[2),3)]:

$$\frac{d\sigma_T}{d\Omega^*} = \frac{\alpha^2 p^*}{W^3} \cdot \frac{m^4 + p^{*4}\sin^4\theta^*}{\left(\frac{W^2}{4} - p^{*2}\cos^2\theta^*\right)^2} \tag{5.23}$$

and we get [Eq. (5.9)]

$$\frac{d\sigma}{dx} = K(s,x)\,\sigma_T$$

with

$$\sigma_T = \frac{4\pi\alpha^2}{W^2} \cdot \frac{p^*}{W} \left[1 + \frac{4m^2}{W^2} - \frac{4m^2(W^2 - 2m^2)}{p^* W^3} \log\left(\frac{W}{2m} + \sqrt{\frac{W^2}{4m^2} - 1} \right) \right] \tag{5.24}$$

$p^* = \sqrt{\frac{W^2}{4} - m^2}$.

The magnitude of $d\sigma/dx$ depends on the position of the threshold $W = 2m$. In Fig. 17 we give a few illustrations for $\sqrt{s} = 100$ GeV and different m values. The cross-section is sizeable up to rather high values of the spin zero boson masses. For example, for $m = 20$ GeV $d\sigma/dx$ culminates around 5pb for $x \simeq$ $\simeq 0.43$ (just above the threshold).

Applications can be done for the search of charged Higgs bosons, of scalar quarks or leptons,... as well as of scalar bound states like hadrons as long as the Born terms of Fig. 16 are a good approximation.

Fermion pair: $\gamma e^{\pm} \to f\bar{f}\, e^{\pm}$

The subprocess $\gamma b \to f\bar{f}$ (with $b = \gamma$ or Z) is now given by the diagrams of Fig. 18 whose amplitude is:

$$T^{\mu\tau} = e^2 Q_f\, \bar{u}_f \left[\frac{\gamma^\mu (m + \not{p} - \not{k}) \gamma^\tau (a_f - b_f \gamma^5)}{2p.k} + \frac{\gamma^\tau (a_f^* - b_f^* \gamma^5)(m + \not{k} - \not{p}') \gamma^\mu}{2p'.k} \right] v_f \,. \tag{5.25}$$

In the case of $W^{\pm}$ exchange (which we shall not develop here) only one diagram would exist for each case $\gamma W^+ \to f^+ f'^0$ or $\gamma W^- \to f^- f'^0$. The differential cross-section of $\gamma e^{\pm} \to f\bar{f}\, e^{\pm}$ is given in Appendix D for arbitrary γ and $e^{\pm}$ polarizations and γ or Z^0 exchange. We have already used it for lepton pair production in Section 3d. If one restricts oneself to the case of unpolarized incident photons and quasi-real γ exchange ($a_f = Q_f$, $b_f = 0$), one can use[2),3)] the $\gamma\gamma \to f\bar{f}$ cross-section:

$$\frac{d\sigma_T}{d\Omega^*} = \frac{2\alpha^2 p^* Q_f^4}{W^3} \left[1 + \frac{2p^{*2}}{\frac{W^2}{4} - p^{*2}\cos^2\theta^*} \left(1 - \frac{p^{*2} \sin^4\theta^*}{\frac{W^2}{4} - p^{*2}\cos^2\theta^*} \right) \right] \tag{5.26}$$

and one gets

$$\frac{d\sigma}{dx} = K(s,x)\, \sigma_T$$

with

$$\sigma_T = \frac{4\pi\alpha^2 Q_f^4}{W^2} \left[-\frac{2p^*}{W} \left(1 + \frac{4m^2}{W^2} \right) + 2 \left(1 + \frac{4m^2}{W^2} - \frac{8m^4}{W^4} \right) \log \left(\frac{W}{2m} + \sqrt{\frac{W^2}{4m^2} - 1} \right) \right]. \tag{5.27}$$

Several numerical examples are illustrated in Fig. 19. The cross-section is higher than the one for spin zero pair production especially for very light particles for which the term $\log W/m$ dominates (it vanishes in the case of a light spin zero pair). For $m = 20$ GeV the fermion pair production cross-section $d\sigma/dx$ culminates around 20pb for $x = 0.48$. We have here a way of producing any kind of new fermion pairs, heavy lepton pairs, heavy quark pairs, etc.

6. - SEARCHES FOR NEW CURRENTS AND PARTICLES

In this section we study several simple channels $\gamma e \to B + F$ which seem particularly interesting for the search for new currents and particles. The bosons B can represent normal states like γ, Z, $W^{\pm}$ or hadrons as well as new states like Higgs bosons (neutral or charged), scalar leptons, scalar quarks, new composite states like pseudo-Goldstone bosons, etc. The fermions F can also be normal leptons like $e^{\pm}$ or ν_e and others as well as new fermionic states like heavy leptons, supersymmetric partners of gauge bosons or of Higgs bosons, excited states, etc. Such particles are predicted to exist in various models based on unified theories[19], supersymmetry[20] or subconstituents[21]. There already exist lower limits for the masses of such objects. They come from the absence of signals in e^+e^- annihilation at Petra and Pep energies[22]. In the case of elementary charged particles (bosons like charged Higgs bosons or supersymmetric scalar leptons or fermions like heavy leptons or excited leptons) the absence of pair production in e^+e^- annihilation via one photon gives a lower limit of the order of 15 GeV. In other cases, the limits depend both on the masses and the coupling constants; these are, for example, the cases of neutral heavy leptons, technipions, single excited lepton effects,... . In these cases one generally concludes that if the corresponding dimensionless coupling constant has a standard magnitude, the masses should be larger than a few GeV[22]. This leaves room for many possibilites in high energy $\gamma e^{\pm}$ collisions.

We develop the following study for the case of direct $\gamma e^{\pm}$ collisions and it is extensible to e^+e^- inelastic scattering as explained before. We decompose this study into five parts.

We start by the neutral spin zero particle production $\gamma e^{\pm} \to B^0 e^{\pm}$ or $\gamma e^{\pm} \to$ $\to B^0 F^{\pm}$ (where $F^{\pm} \neq e^{\pm}$ is a heavy fermion). The first case would occur if the diagonal eeB^0 coupling exists with a reasonable magnitude, if not, one still has the second possibility.

We then consider the charged case $\gamma e^{\pm} \to B^{\pm}\nu_e$ or $\gamma e^{\pm} \to B^{\pm}F^0$ requiring $e^{\pm}\nu_e B^{\pm}$ or $e^{\pm}F^0B^{\pm}$ couplings, F^0 being a new neutral fermion.

We then develop the description of more general processes going through one fermion formation, one fermion exchange or one scalar boson exchange. New fermion (f) formation in $\gamma e^{\pm}$ collisions could appear if there is an appreciable γef coupling (this generalizes the case of e^* formation). New fermion exchange may occur even if there is no γef coupling, but if γfF and efB couplings exist,

f, F and B being two different fermions and one new boson. Scalar (S) boson exchange (with S neutral or charged) will occur if there are γSB and eFS couplings (S and B on the one hand and e and F on the other being identical or not). This may be interesting when there is no appreciable $\gamma\gamma B$ coupling allowing for a more copious B production.

6a. Neutral spin zero particle production $\gamma e^{\pm} \to B^0 f^{\pm}$

This process is described by the diagrams of Fig. 20. The formulae apply to both cases whether f is an electron or not. The γee and γff couplings are standard QED ones. We take the efB^0 couplings as

$$L = e\,\bar{\psi}_e (c - i d\gamma^5)\,\psi_f\,\phi_B + h.c. \tag{6.1}$$

(again C invariance holds if c and d are real, but CP invariance holds if c is real and d is purely imaginary), and one gets:

$$\begin{aligned}
\frac{d\sigma}{d\Omega} = \frac{\alpha^2 p}{s\sqrt{s}} \Bigg\{ & \Big[(|c|^2+|d|^2)(1+\bar{\lambda}P_L) - 2Q_e(\bar{\lambda}+P_L)\,\mathrm{Im}\,cd^*\Big]\frac{m_f^2-u}{2s} \\
& + \frac{1}{(u-m_f^2)^2}\Bigg[\Big[|c|^2+|d|^2-2Q_eP_L\,\mathrm{Im}\,cd^*\Big]\Big(\frac{s}{2}(m_f^2-u)+(u-m_B^2)p^2\sin^2\theta\,(1+\xi_3\cos 2\varphi-\xi_1\sin 2\varphi)\Big) \\
& \quad - s\bar{\lambda}m_f p P_\perp \sin\theta\Big[2\,\mathrm{Re}\,cd^*\sin(\beta-\varphi) - (|c|^2-|d|^2)\cos(\beta-\varphi)\Big] \\
& \quad - \frac{\bar{\lambda}}{4}Q_e\Big[2\,\mathrm{Im}\,cd^* - Q_eP_L(|c|^2+|d|^2)\Big]\Big((m_f^2-u)(m_f^2-t)+(u-m_B^2)(u-3m_f^2)\Big)\Bigg] \\
& + \frac{1}{s(u-m_f^2)}\Bigg[\Big[|c|^2+|d|^2-2Q_eP_L\,\mathrm{Im}\,cd^*\Big]\Big(s(m_f^2-u)-sp^2\sin^2\theta\,(1+\xi_3\cos 2\varphi-\xi_1\sin 2\varphi)\Big) \\
& \quad - s\bar{\lambda}m_f p P_\perp \sin\theta\Big[2\,\mathrm{Re}\,cd^*\sin(\beta-\varphi) - (|c|^2-|d|^2)\cos(\beta-\varphi)\Big] \\
& \quad - \bar{\lambda}Q_e\Big[2\,\mathrm{Im}\,cd^* - Q_eP_L(|c|^2+|d|^2)\Big]\Big(sm_f^2-(u-m_B^2)(m_f^2-u)\Big)\Bigg]\Bigg\}
\end{aligned} \tag{6.2}$$

The $e^{\pm}$ and γ longitudinal polarizations control the C violating terms and the $e^{\pm}$ transverse polarizations with γ circular polarizations control the other $\mathrm{Re}\,cd^*$ and $(|c|^2 - |d|^2)$ combinations.

In the unpolarized case the cross-section depends only on $(|c|^2 + |d|^2)$. The integrated cross section becomes:

$$\sigma = \frac{2\pi\alpha^2 p(|c|^2+|d|^2)}{s^2}\left[2B^0 - 5p^0 + \frac{s+4p^0(p^0-B^0)}{p}\log\frac{p+p^0}{m_f}\right] \qquad (6.3)$$

with

$$p^0 = \frac{s+m_f^2-m_B^2}{2\sqrt{s}} \quad , \quad B^0 = \sqrt{s} - p^0 \ .$$

In Fig. 21 we illustrate this result, factorizing out $(|c|^2 + |d|^2)$ which is dimensionless and could be of order one if the couplings are first order allowed ones. One can discuss two extreme cases.

First, if $f^\pm \equiv e^\pm$ (i.e., $\gamma e^\pm \to B^0 e^\pm$) one has a situation comparable to $\gamma e \to Ze$ with a strong backward peaking due to the electron exchange diagram and consequently the log term is important in σ. The cross-section is then rather large even for very massive B^0 bosons:

$$R \simeq 10\,(|c|^2+|d|^2)$$

for $m_{B^0} \simeq 10$ to 40 GeV.

If $f^\pm$ is a heavy fermion, the situation is obviously different - the log term is inefficient, the backward peaking is small and the level of the cross-section is weaker, i.e., $R \simeq (|c|^2 + |d|^2)$, which will be of order one for standard couplings.

6b. Charged spin zero particle production: $\gamma e^\pm \to B^\pm f^0$

We now have t channel and s channel diagrams of Fig. 22. The neutral fermion f^0 can be either a (massless) neutrino ν_e or a heavy neutral lepton. We use the QED $\gamma B^\pm B^\pm$ couplings and the same form of efB couplings as in the neutral case. The resulting cross-section is:

$$\frac{d\sigma}{d\Omega} = \frac{\alpha^2 p}{s\sqrt{s}}\left\{\left[|c|^2+|d|^2-2\varphi_e P_L\,\mathrm{Im}\,cd^*\right]\frac{m_f^2-t}{(m_B^2-t)^2}\,p^2\sin^2\theta\,(1+\xi_3\cos 2\varphi - \xi_1\sin 2\varphi)\right.$$

(6.4)

$$+\left[(|c|^2+|d|^2)(1+\bar\lambda P_L)-2Q_e\,\mathrm{Im}\,cd^*(\bar\lambda+P_L)\right]\frac{m_f^2-u}{2s}$$

$$+\frac{1}{s(t-m_B^2)}\Big[\left[|c|^2+|d|^2-2Q_eP_L\,\mathrm{Im}\,cd^*\right]sp^2\sin^2\theta\,(1+\xi_3\cos2\varphi-\xi_3'\sin2\varphi)$$
$$+s\bar\lambda m_f p P_L\sin\theta\,(2\,\mathrm{Re}\,cd^*\sin(\beta-\varphi)-(|c|^2-|d|^2)\cos(\beta-\varphi))$$
$$-\bar\lambda Q_e\left[2\,\mathrm{Im}\,cd^*-Q_eP_L(|c|^2+|d|^2)\right](ut-m_B^2m_f^2)\Big]\Big\}. \qquad (6.4)\ \text{cont.}$$

The polarization structure of $d\sigma/d\Omega$ is comparable to that of the neutral case. We now have linear γ polarization associated with the t channel boson exchange diagram.

In the unpolarized case the integrated cross-section becomes:

$$\sigma=\frac{2\pi\alpha^2p(|c|^2+|d|^2)}{s\sqrt{s}}\left[\frac{p^0}{\sqrt{s}}+\frac{4(m_f^2-m_B^2)}{s}\left(\frac{B^0}{p}\,\mathrm{Log}\,\frac{p+B^0}{m_B}-1\right)\right] \qquad (6.5)$$

(same notations as in the neutral case). Illustrations are given in Fig. 23. The light fermion case ($f^0\equiv\nu_e$) no longer has any special property. The angular distribution is slightly peaked forward if m_B is not too high; but as we do not know any light boson $B^\pm$ the corresponding log term is less important than in the preceding neutral case with a light fermion. The cross-section is then at most of the order of $R\simeq(|c|^2+|d|^2)$.

6c. More general fermion formation processes

We already considered the case of e^* formation in $\gamma e\to e^*\to\gamma e$ in Section 3b. We now treat a more general case, $\gamma e\to f\to$ final state (F), see Fig. 24.

We again use the general gauge invariant γef coupling

$$L=\frac{e}{2}\bar\psi_f\sigma^{\mu\nu}(a-ib\gamma^5)\psi_eF_{\mu\nu}+\text{h.c.} \qquad (6.6)$$

We write the general form of the fermion propagator correction factor $f\to(F)\to f$ as:

$$\sigma_f=A-B\gamma^5+(C-D\gamma^5)(\not q-m_f) \qquad (6.7)$$

and for the antifermion:

$$\mathcal{O}_{\bar{f}} = -\bar{A} + \bar{B}\gamma^5 + (\not{q} + m_f)(\bar{C} + \bar{D}\gamma^5) \tag{6.8}$$

with a priori no symmetry relation between ABCD and $\bar{A}\bar{B}\bar{C}\bar{D}$.

The resulting integrated cross-section of $\gamma e \to f \to (F)$ is then:

$$\sigma = \frac{2\pi\alpha s}{|D_f|^2}\left\{(1+\bar{\lambda}P_L)\left[(|a|^2+|b|^2)(2m_f A + C(s-m_f^2)) + 2(\mathrm{Im}\, ab^*)D(s-m_f^2)\right]\right.$$
$$\left. + Q_e(\bar{\lambda}+P_L)\left[(|a|^2+|b|^2)D(s-m_f^2) + 2(\mathrm{Im}\, ab^*)(2m_f A + C(s-m_f^2))\right]\right\} \tag{6.9}$$

where $(A,\ldots)$ should be replaced by $(\bar{A},\ldots)$ in the case of positrons; and $|D_f|^2 = (s-m_f^2)^2 + m_f^2\Gamma_f^2$. The partial width $\Gamma_{f\to F}$ is given by:

$$\Gamma_{f\to F}(s) = A + \frac{C}{m_f}(s-m_f^2) \ . \tag{6.10}$$

Notice that the total widths Γ_f and $\Gamma_{\bar{f}}$ (summed over all F states) are equal due to CPT invariance, but this is not necessarily the case for partial widths if C or CP are not conserved. The polarized partial width $\Gamma_{f\to e\gamma}$ is:

$$\Gamma_{f\to e\gamma} = \frac{\alpha m_f^3}{8}\left[(|a|^2+|b|^2)(1+\bar{\lambda}P_L) + 2Q_e(\mathrm{Im}\, ab^*)(\bar{\lambda}+P_L)\right] \ . \tag{6.11}$$

In the vicinity of $s = m_f^2$ and in the unpolarized case one recovers the Breit-Wigner form:

$$\sigma = \frac{8\pi}{s}\cdot\frac{m_f\Gamma_{f\to F}\, m_f\Gamma_{f\to e\gamma}}{|D_f|^2} \tag{6.12}$$

with

$$\Gamma_{f\to e\gamma} = \frac{\alpha m_f^3}{8}(|a|^2+|b|^2) \ .$$

The cross-section at the peak $\sigma^{\mathrm{peak}} \simeq (8\pi/s)B_{f\to e\gamma}B_{f\to F}$ corresponds to a value of R equal to:

$$R^{\mathrm{peak}} \simeq \frac{6}{\alpha^2}B_{f\to e\gamma}$$

if one sums over the dominant F channels. For example, one reaches $R^{\mathrm{peak}} \simeq 1$ if the $e\gamma$ branching ratio reaches $B_{f\to e\gamma} \simeq 10^{-5}$.

If f is a narrow state one may use the expression of the integrated spectrum around $s = m_f^2$:

$$\bar{\sigma} = \int \sigma \, d\sqrt{s} \simeq \frac{4\pi^2}{m_f^2} \Gamma_{f \to e\gamma} \quad . \tag{6.13}$$

The measurability of $\bar{\sigma}$ depends on the energy resolution Δ of the $e^{\pm}$ and γ beams. $\bar{\sigma}$ is comparable to an $R = 1$ flat background when

$$\Gamma_{f \to e\gamma} = \frac{m_f^2}{4\pi^2} \sigma_0 \Delta$$

For $m_f = 100$ GeV and $\Delta = 1$ GeV one needs $\Gamma_{f \to e\gamma} = 5$ keV.

Equation (6.9) for the cross-section can be applied to any kind of final state F for which the quantities A, B, C, D can be computed. For example, in the case $\gamma e \to e^* \to \gamma e$ of Section 3c one has:

$$A = \bar{A} = C m_f \quad , \quad C = \bar{C} = \frac{\alpha s}{2}(|a|^2 + |b|^2) \quad , \quad D = \bar{D} = \alpha s \, \mathrm{Im} ab^* \quad . \tag{6.14}$$

In the unpolarized case, σ only measurés the C conserving combinations; longitudinal polarizations are needed in order to be sensitive to C violating terms.

We give another example with the decay of the new fermion f into spin 0 and spin 1/2 states (Fig. 25). Using the fBf' coupling

$$L = e \, \bar{\psi}_{f'} (c - i d \gamma^5) \psi_f + h.c. \tag{6.15}$$

(again one has C invariance if c and d are real but CP invariance if c is real but d purely imaginary) one gets the differential cross-section

$$\begin{aligned} \frac{d\sigma}{d\Omega} = \frac{\alpha^2 p}{\sqrt{s} |D_f|^2} \Big\{ & \left[(|a|^2 + |b|^2)(1 + \bar{\lambda} P_L) + 2 Q_e \, \mathrm{Im} ab^* (\bar{\lambda} + P_L) \right] \left[m_f m_{f'} s (|c|^2 - |d|^2) + (s q \cdot f' + (m_f^2 - s) k \cdot f')(|c|^2 + |d|^2) \right] \\ & + Q_e \, \mathrm{Im} cd^* \left[(|a|^2 + |b|^2)(\bar{\lambda} + P_L) + 2 Q_e \, \mathrm{Im} ab^* (1 + \bar{\lambda} P_L) \right] (2 k \cdot f' (s + m_f^2) - 2 s q \cdot f' \\ & + 2 m_f s Q_e \, \mathrm{Im} cd^* P_\perp \sin\theta \left[(|a|^2 - |b|^2)(\xi_3 \cos(\beta + \phi) - \xi_1 \sin(\beta + \phi)) \right. \\ & \left. - (|a|^2 + |b|^2)(\xi_3 \sin(\beta + \phi) + \xi_1 \cos(\beta + \phi)) \right] \Big\} . \end{aligned} \tag{6.16}$$

Notice the $e^{\pm}$ transverse and γ linear polarization dependences associated with m_f mass terms and the C violating terms Imab* and Imcd* The integrated cross-section can be written in the form of Eq. (6.9) with

$$A=\overline{A}=Cm_f+\frac{\alpha f'm_{f'}}{\sqrt{s}}(|c|^2-|d|^2) \qquad C=\overline{C}=\frac{\alpha f'f'^0}{s}(|c|^2+|d|^2)$$
$$D=\overline{D}=-\frac{\alpha f'f'^0}{s}2\,\mathrm{Im}\,cd^* . \tag{6.17}$$

6d. More general fermion exchange processes

Here we consider the reaction $\gamma e \to F + B$ where a fermion f (different from F) is exchanged (Fig. 26). We again use the γfF couplings

$$L=\frac{e}{2}\overline{\psi}_F\sigma^{\mu\nu}(a'-ib'\gamma^5)\psi_f F_{\mu\nu}+h.c. \tag{6.18}$$

and in the case of spin zero B^0 particle the efB^0 couplings:

$$L=e\,\overline{\psi}_e(c-id\gamma^5)\psi_f\phi_B+h.c. \tag{6.19}$$

The formulae given below apply to the cases where $f^{\pm}$ is either different from or identical to $e^{\pm}$.

$$\frac{d\sigma}{d\Omega}=\frac{\alpha^2\beta(m_F^2-u)}{s\sqrt{s}(m_f^2-u)^2}\left\{\left[|a'|^2+|b'|^2+2\lambda Q_e\,\mathrm{Im}\,a'b'^*\right]\left[|c|^2+|d|^2-2Q_eP_L\,\mathrm{Im}\,cd^*\right]\frac{sm_f^2+ut-m_F^2m_B^2}{2}\right.$$
$$+\left[2Q_e\,\mathrm{Im}\,a'b'^*+\lambda(|a'|^2+|b|^2)\right]\left[\left(-2Q_e\,\mathrm{Im}\,cd^*+P_L(|c|^2+|d|^2)\right)\frac{sm_f^2-ut+m_F^2m_B^2}{2}\right.$$
$$\left.\left.+sm_f\beta P_T\sin\theta\left(\mathrm{Re}\,cd^*\sin(\varphi-\beta)+(|c|^2-|d|^2)\cos(\varphi-\beta)\right)\right]\right\} \tag{6.20}$$

Notice the absence of γ linear polarization terms but the presence of $e^{\pm}$ transverse polarization terms associated with m_f.

If the exchanged fermion f is a heavy one, the cross-section has a standard magnitude, i.e., $R\approx\left[(|a'|^2+|b'|^2)(|c|^2+|d|^2)\pm 4\,\mathrm{Im}\,a'b'^*+\mathrm{Im}\,cd^*\right]M^2$ (a' and b' have dimension M^{-1}; M is some heavy mass scale). If the exchanged fermion $f^{\pm}$ is the $e^{\pm}$, i.e., if the γeF and eeB^0 couplings exist, the cross-section is obviously larger by the factor $\log s/m_e^2$ corresponding to the backward peaking. Notice that in these cases one should independently observe the B^0 production through the process $\gamma e \to eB^0$ of Section 6a and the $F^{\pm}$ formation $\gamma e^{\pm} \to F^{\pm}$ of Section 6c.

6e. More general scalar boson exchange processes

We can develop the formalism of scalar boson exchange (Fig. 27) in a way similar to the case of vector boson exchange treated in Section 5. We again take the lower efS vertex as given by $L = e\bar{\psi}_e (c - id\gamma^5)\psi_F \phi_S + h.c.$ (for charged or neutral S exchange) with F being a massive or a massless fermion identical or not to e or ν_e.

The upper γS collision amplitude is written $\varepsilon^\mu T_\mu$ and corresponds to the cross-section:

$$\sigma^{\gamma b}(\lambda\lambda') = \frac{(2\pi)^4}{4k^* W} E^{\mu\nu} M_{\mu\nu} \tag{6.21}$$

with $$M_{\mu\nu} = \int dp_B \, T_\mu T_\nu^*$$

and $$M(\lambda\lambda') = \varepsilon^\mu(\lambda)\, \varepsilon^{\nu *}(\lambda')\, M_{\mu\nu}$$

The final fermion spectrum now has the general form:

$$\frac{\ell'^0 d\sigma}{d_3 \ell'} = \frac{\pi e^2 (m_F^2 - t)}{2s\,|D(k')|^2} \left[|c|^2 + |d|^2 - 2Q_e P_L \, \mathrm{Im} cd^*\right] E^{\mu\nu} M_{\mu\nu} \tag{6.22}$$

$$|D(k')|^2 = \left(k'^2 - m_S^2\right)^2$$

or

$$\frac{d\sigma}{dW^2 d\Omega} = \frac{e^2 k^* \ell' W (m_F^2 - t)}{2(2\pi)^3 s\sqrt{s}\,|D(k')|^2} \left[|c|^2 + |d|^2 - 2Q_e P_L \, \mathrm{Im} cd^*\right] \sum_{\lambda\lambda'} E(\lambda\lambda')\, \sigma^{\gamma b}(\lambda\lambda') . \tag{6.23}$$

In the case of a single boson production ($\gamma S \to B$) we can use the decay correlation:

$$\gamma(\lambda\lambda') = \frac{k^*}{8\pi M_B^2 (2J+1)} \varepsilon^\mu(\lambda)\, \varepsilon^{\nu *}(\lambda')\, T_\mu T_\nu^* \tag{6.24}$$

and write the final fermion angular distribution:

$$\frac{d\sigma}{d\Omega} = \frac{(2J+1) e^2 M_B^2 \ell' (m_F^2 - t)}{4\pi k^* s\sqrt{s}\,|D(k')|^2} \left[|c|^2 + |d|^2 - 2Q_e P_L \, \mathrm{Im} cd^*\right] \sum_{\lambda\lambda'} E(\lambda\lambda')\, \gamma(\lambda\lambda') \tag{6.25}$$

where $\gamma(\lambda\lambda)$ coincides with the polarized decay width $\Gamma_{B\to\gamma S}(\lambda)$ when averaged over angles.

The case where the final boson B is a spin zero particle exists only if B is charged (there is no $\gamma S^0 B^0$ coupling for spin zero particles). We have already treated this case in Section 6c with its gauge invariance constraint.

We now treat the case where B is a spin one particle. In the general form (without parity conservation) the γSB vertex is written:

$$e\left\{ig\,\varepsilon^{\mu\nu\rho\sigma}\varepsilon_\mu k_\nu e^*_\rho p_{B\sigma} + g'(\varepsilon.e^*k.p_B - \varepsilon.p_B e^*.k)\right\}. \qquad (6.26)$$

The resulting cross-section is:

$$\frac{d\sigma}{d\Omega} = \frac{\alpha^2 \ell'(m_F^2-t)(m_B^2-t)}{8s\sqrt{s}\,(m_S^2-t)^2}\left[|c|^2+|d|^2-2Q_e P_L\,\mathrm{Im}\,cd^*\right]\left[|g|^2+|g'|^2+2\bar{\lambda}\,\mathrm{Re}\,gg'^*\right]. \qquad (6.27)$$

If the exchanged scalar S particle is a heavy one (light ones would already have been seen in e^+e^- collisions) the angular distribution will almost be isotropic when m_S, m_F and m_B have comparable values. The integrated cross-section will then be of standard magnitude, i.e., $R \simeq (|c|^2 + |d|^2)(|g|^2 + |g'|^2)$ in the unpolarized case. Longitudinal $e^\pm$ polarizations can measure C violating terms $\mathrm{Im}\,cd^*$ at the eFS vertex. With parity conservation at the γSB vertex one only has the g coupling if $P_S = P_B$ and only g' if $P_S = -P_B$ and hence no γ helicity dependence. This formula applies to the case where B is a neutral or charged elementary or composite spin one boson.

ACKNOWLEDGMENTS

We thank M. Jacob and J. Prentki for reading the manuscript and for their comments and suggestions.

APPENDIX A: NOTATIONS

We use the metric $g^{\mu\nu}$ ($g^{00} = +1$, $g^{ii} = -1$; $i = 1,2,3$) and the anti-symmetric tensor $\varepsilon^{\mu\nu\rho\sigma}$ ($\varepsilon^{0123} = +1$). Dirac matrices are

$$\gamma^0 = \begin{pmatrix} I & 0 \\ 0 & -I \end{pmatrix} \qquad \gamma^i = \begin{pmatrix} 0 & \sigma^i \\ -\sigma^i & 0 \end{pmatrix} \qquad \gamma^5 = i\gamma^0\gamma^1\gamma^2\gamma^3 = \begin{pmatrix} 0 & I \\ I & 0 \end{pmatrix} .$$

Other notations for fields and couplings are standard ones [see, for example, Ref. 2)] .

For gauge boson couplings with fermions we take the standard form:

$$L = -e\,\bar{\psi}\,\gamma^\mu (a_f - b_f \gamma^5)\,\psi\, A_\mu \qquad (A.1)$$

with

$a_f = Q_f$, $b_f = 0$ for the photon

a_f and b_f given in Table 1 for the Z

$$a_f = b_f = \frac{1}{2\sqrt{2}\sin\theta_W} \quad \text{for } W^\pm$$

We use $\sin^2\theta_W = 0.215$ in numerical applications. For γW^+W^- or ZW^+W^- vertices we take the Yang-Mills form:

$$L = eg\left[g^{\tau\mu}(-p'-q)^\rho + g^{\mu\rho}(p+q)^\tau + g^{\tau\rho}(-p+p')^\mu\right] A_\mu(q)\, W_\tau^+(p')\, W_\rho^-(p) \qquad (A.2)$$

$A_\mu(q)$, $W_\tau^+(p')$, $W_\rho^-(p)$ being polarization vectors of incoming γ or Z and outgoing $W^\pm$ bosons; $g = 1$ for the γ and $\cot g\theta_W$ for the Z.

APPENDIX B: TECHNICAL DETAILS FOR BOSON EXCHANGE PROCESSES

In Section 5 we considered the reaction $\gamma e^{\pm} \to (B) + F$ where F is a light fermion ($e^{\pm}$ or ν_e) with momentum ℓ' and (B) a bosonic state with invariant mass W. This reaction is supposed to proceed by the exchange of a boson b in the t channel. We define the γb c.m. frame depicted in Fig. 28b; γb c.m. variables will generally be labelled by a star. The b momentum is along the Oz axis: $k'^{\mu} = (k'^{0*}, 0, 0, k^*)$ and the γ momentum is opposite it: $k^{\mu} = (k^*, 0, 0, -k^*)$. The Oxz plane contains $\vec{k}^*$, $\vec{k}'^*$, $\vec{\ell}^*$ and $\vec{\ell}'^*$ momenta with angles θ^* between $\vec{\ell}^*$ and $\vec{\ell}'^*$ and α^* between $\vec{k}'^*$ and $\vec{\ell}'^*$. Useful relations (needed for exploiting Table 2) are:

$$\ell'^* = \ell' \frac{\sqrt{s}}{W} \qquad k^* = \frac{k(1-v\cos\theta)}{\sqrt{1-v^2}} \qquad k^* \sin\alpha^* = k \sin\theta \qquad k^* \cos\alpha^* = \frac{k(\cos\theta - v)}{\sqrt{1-v^2}}$$

$$k'^{0*} = \frac{k'^0 + k' v \cos\alpha}{\sqrt{1-v^2}} \qquad k'^* \cos\alpha^* = \frac{k' \cos\alpha + v k'^0}{\sqrt{1-v^2}} \qquad k'^* \sin\alpha^* = k' \sin\alpha$$

with

$$v = \frac{\ell'}{\sqrt{s} - \ell'^0} \qquad \sqrt{1-v^2} = \frac{W}{\sqrt{s} - \ell'^0} \qquad \cos\alpha = \frac{\ell \cos\theta - \ell'}{k'} \qquad \cos\alpha^* = \frac{\cos\theta - v}{1 - v\cos\theta} .$$

In this γb c.m. we should use the boson b and photon helicity states:

$$e^{\mu}(h) = \varepsilon^{\mu}(-h) = \left(0, -\frac{h}{\sqrt{2}}, \frac{-i}{\sqrt{2}}, 0\right) \quad \text{for } h = \pm 1$$

$$e^{\mu}(0) = \left(\frac{k'^*}{\sqrt{-k'^2}}, 0, 0, \frac{k'^{0*}}{\sqrt{-k'^2}}\right) \quad \text{for } h = 0 .$$

These states are normalized to

$$\varepsilon^{\mu *}(h)\, \varepsilon_{\mu}(h) = e^{\mu *}(h)\, e_{\mu}(h) = N_h = -1 \quad \text{for } h = \pm 1$$

and

$$e^{\mu *}(0)\, e_{\mu}(0) = N_0 = +1 \quad \text{for } h = 0$$

The transformation of the γe c.m. frame (Fig. 28a) into the γb c.m. frame (Fig. 28b) contains a rotation of azimuthal angle ϕ around OZ, a boost along $\vec{\ell}'$ in order to bring (B) to rest and a rotation of angle $(\alpha^* - \theta^*)$ around the normal to the Oxz plane in order to bring the Oz axis from $\vec{\ell}^*$ to $\vec{k}'^*$.

As a result we have, in terms of γb c.m. helicity states,

$$E(\lambda\lambda') = \varepsilon^{\mu *}(\lambda) \varepsilon^{\nu}(\lambda')\, E_{\mu\nu} = \frac{1}{2}\left\{ \delta_{\lambda\lambda'} + \frac{\xi_3}{2}\left[\cos 2\phi\,(\lambda\lambda' - 1) + i(\lambda - \lambda')\sin 2\phi\right]\right. \quad \text{(B.1)}$$

$$+\frac{\xi_1}{2}\left[(1-\lambda\lambda')\sin 2\varphi + i(\lambda-\lambda')\cos 2\varphi\right] + \frac{\xi_2}{2}(\lambda+\lambda')\Big\}\cdot \qquad \text{(B.1) cont.}$$

The elements of the leptonic vertex $L(\eta\eta')$ defined in Section 5 are calculated in this γb frame:

$$L(bb') = N_b N_{b'} e^{\tau\alpha}(b) e^{\tau'}(b') L_{\tau\tau'}$$

$$= \left[|a|^2+|b|^2+2Q_e P_L \mathrm{Re}ab^*\right] U(bb') - \left[P_L(|a|^2+|b|^2)+2Q_e \mathrm{Re}ab^*\right]\Sigma(bb') \qquad \text{(B.2)}$$

with $U(\eta\eta')$ and $\Sigma(\eta\eta')$ given in Table 2.

APPENDIX C: COMPLETE e^* EFFECT IN COMPTON SCATTERING

$$
\begin{aligned}
\frac{d\sigma}{d\Omega} = \frac{\alpha^2}{2s}\Bigg\{ & \frac{t}{u}(1+\bar\lambda P_L) + \frac{t}{s}(1-\bar\lambda P_L) + 2 \\
& + \frac{2s(s-M^2)}{|D_s|^2}\Big(s\left[|a|^2+|b|^2+2Q_e P_L\, \mathrm{Im}ab^*\right] + (t-u)\bar\lambda\left[P_L(|a|^2+|b|^2)+2Q_e\,\mathrm{Im}ab^*\right]\Big) \\
& + \frac{2u}{u-M^2}\Big(u\left[|a|^2+|b|^2+2Q_e P_L\,\mathrm{Im}ab^*\right] - t\bar\lambda\left[P_L(|a|^2+|b|^2)+2Q_e\,\mathrm{Im}ab^*\right]\Big) \\
& - \frac{2s^2M^2\Gamma}{|D_s|^2}pP_T\sin\theta\Big(2\,\mathrm{Re}ab^*\left[\xi_3\cos(\beta+\phi)-\xi_1\sin(\beta+\phi)\right]+(|a|^2-|b|^2)\left[\xi_3\sin(\beta+\phi)+\xi_1\cos(\beta+\phi)\right]\Big) \\
& - \frac{s^2}{|D_s|^2}\Big((|a|^2+|b|^2)(su+tM^2)\left[(|a|^2+|b|^2)(1+\bar\lambda P_L)+2Q_e(\bar\lambda+P_L)\,\mathrm{Im}ab^*\right] \\
& \qquad +2Q_e\,\mathrm{Im}ab^*(su-tM^2)\left[(|a|^2+|b|^2)(\bar\lambda+P_L)+2Q_e(1+\bar\lambda P_L)\,\mathrm{Im}ab^*\right] \\
& \qquad +8Q_e\,\mathrm{Re}ab^*\,\mathrm{Im}ab^*\,sMpP_T\sin\theta\left[\xi_3\sin(\beta+\phi)+\xi_1\cos(\beta+\phi)\right] \\
& \qquad -4Q_e(|a|^2-|b|^2)\,\mathrm{Im}ab^*\,sMpP_T\sin\theta\left[\xi_3\cos(\beta+\phi)-\xi_1\sin(\beta+\phi)\right]\Big) \\
& - \frac{u^2}{(u-M^2)^2}\Big((us-tM^2)\left[2Q_e\,\mathrm{Im}ab^*+P_L(|a|^2+|b|^2)\right]\left[2Q_e\,\mathrm{Im}ab^*+\bar\lambda(|a|^2+|b|^2)\right] \\
& \qquad -(us+tM^2)\left[|a|^2+|b|^2+2Q_eP_L\,\mathrm{Im}ab^*\right]\left[|a|^2+|b|^2+2Q_e\bar\lambda\,\mathrm{Im}ab^*\right]\Big) \\
& + \frac{2sM(s-M^2)}{(u-M^2)|D_s|^2}\Big(Mt\left[(t-s)\bar\lambda P_L-u\right]\left[(|a|^2+|b|^2)^2-4\,(\mathrm{Im}ab^*)^2\right] \\
& \qquad -4Q_e\,\mathrm{Im}ab^*\,\mathrm{Re}ab^*\,usp\,P_T\sin\theta\left[\xi_3\sin(\beta+\phi)+\xi_1\cos(\beta+\phi)\right] \\
& \qquad -(|a|^4-|b|^4)sp\,P_T\sin\theta\Big(s\left[\xi_3\cos(\beta+\phi)-\xi_1\sin(\beta+\phi)\right]+t\left[\cos(\beta-\phi)+\xi_3\cos(\beta+\phi)\right. \\
& \qquad\qquad \left.-\xi_1\sin(\beta+\phi)\right]\Big)\Big) \\
& - \frac{2M^2s^2p\Gamma P_T\sin\theta}{(u-M^2)|D_s|^2}(|a|^2+|b|^2)\Big((|a|^2-|b|^2)u\left[\xi_3\sin(\beta+\phi)+\xi_1\cos(\beta+\phi)\right] \\
& \qquad -2\,\mathrm{Re}ab^*\,t\left[\cos(\beta-\phi)+\xi_3\cos(\beta+\phi)-\xi_1\sin(\beta+\phi)\right]\Big)\Bigg\}
\end{aligned}
$$

$$|D_s|^2 \equiv (s-M^2)^2 + M^2\Gamma^2 \,.$$

APPENDIX D: DIFFERENTIAL CROSS-SECTION OF $\gamma e^{\pm} \to f\bar{f}e^{\pm}$

In the case of γ or Z^0 exchange the differential cross-section obtained by the subprocess of Fig. 18 and Eqs. (5.1) - (5.20) takes the general form:

$$\frac{d\sigma}{dW^2 d\Omega d\Omega^*} = \frac{\alpha^3 p^* \ell' Q_f^2}{4\pi^2 s W \sqrt{s}\, |D(k')|^2} \left[\frac{N}{(k\cdot p)^2} + \frac{N'}{(k\cdot p')^2} + \frac{N''}{k\cdot p\; k\cdot p'} \right] \tag{D.1}$$

with

$$\begin{aligned} N = {} & (a_f^2+b_f^2)\left[(a^2+b^2+2ab\,Q_e P_L)\, S^{\mu\nu} L^{\rho\sigma} X^1_{\mu\nu\rho\sigma} - (2ab\,Q_e + P_L(a^2+b^2))\, A^{\mu\nu}\Sigma^{\rho\sigma} Y^1_{\mu\nu\rho\sigma}\right] \\ & - m^2(a_f^2-b_f^2)\left[(a^2+b^2+2ab\,Q_e P_L)\, S^{\mu\nu} p_\mu p_\nu (-2\ell\cdot\ell') - 2(2ab\,Q_e + P_L(a^2+b^2))\, A^{\mu\nu}\Sigma^{\rho\sigma} p_\mu k_\rho g_{\nu\sigma}\right] \\ & + 2a_f b_f \left[(a^2+b^2+2ab\,Q_e P_L)\, A^{\mu\nu} L^{\rho\sigma} X^2_{\mu\nu\rho\sigma} + (2ab\,Q_e + P_L(a^2+b^2))\, S^{\mu\nu}\Sigma^{\rho\sigma} Y^2_{\mu\nu\rho\sigma}\right] \end{aligned} \tag{D.2}$$

$$N' = N\,(p \leftrightarrow p',\; b_f \leftrightarrow -b_f)$$

$$\begin{aligned} N'' = {} & (a_f^2+b_f^2)\left[(a^2+b^2+2ab\,Q_e P_L)\, S^{\mu\nu} L^{\rho\sigma} X^3_{\mu\nu\rho\sigma} - (2ab\,Q_e + P_L(a^2+b^2))\, A^{\mu\nu}\Sigma^{\rho\sigma} Y^3_{\mu\nu\rho\sigma}\right] \\ & + m^2(a_f^2-b_f^2)\left[(a^2+b^2+2ab\,Q_e P_L)(-4\ell\cdot\ell' S^{\mu\nu} p_\mu p_\nu - L^{\rho\sigma} k_\rho k_\sigma)\right. \\ & \left. - 2(2ab\,Q_e + P_L(a^2+b^2))(A^{\mu\nu}\Sigma^{\rho\sigma}(p_\mu k_\rho g_{\nu\sigma} - p'_\nu k_\rho g_{\mu\sigma}))\right] \\ & - 2a_f b_f \left[(a^2+b^2+2ab\,Q_e P_L)\, A^{\mu\nu} L^{\rho\sigma} X^4_{\mu\nu\rho\sigma} + (2ab\,Q_e + P_L(a^2+b^2))\, S^{\mu\nu}\Sigma^{\rho\sigma} Y^4_{\mu\nu\rho\sigma}\right] \end{aligned} \tag{D.3}$$

and the tensors

$$\begin{aligned} S^{\mu\nu} &= \frac{1}{2}\left[-g^{\mu\nu} + \frac{q^\mu q^\nu}{s} - n_3^\mu n_3^\nu + \xi_3(Q_{11}^{\mu\nu} - Q_{22}^{\mu\nu}) + \xi_1 Q_{12}^{\mu\nu}\right] \\ A^{\mu\nu} &= \frac{\lambda}{s}\varepsilon^{\mu\nu\rho\sigma} k_\rho q_\sigma \\ L^{\rho\sigma} &= \ell'^\rho \ell^\sigma + \ell^\rho \ell'^\sigma - \ell\cdot\ell' g^{\rho\sigma} \\ \Sigma^{\rho\sigma} &= \varepsilon^{\rho\sigma\alpha\beta} \ell_\alpha \ell'_\beta \end{aligned} \tag{D.4}$$

$$X^1_{\mu\nu\rho\sigma} = k\cdot p\,(2p_\nu p'_\sigma g_{\mu\tau} - p_\mu p'_\nu g_{\rho\sigma} - g_{\mu\nu} k_\rho p'_\sigma + \tfrac{1}{2} k\cdot p' g_{\mu\nu} g_{\rho\sigma}) - 2p_\mu p_\nu q'_\rho p'_\sigma + q'\cdot p' p_\mu p_\nu g_{\rho\sigma}$$

$$X^2_{\mu\nu\rho\sigma} = 2p_\nu p'_\sigma \varepsilon_{\mu\alpha\beta\rho} p^\alpha k^\beta - k\cdot p\, p'_\sigma \varepsilon_{\nu\mu\alpha\rho} k^\alpha - g_{\rho\sigma} p_\nu \varepsilon_{\mu\alpha\beta\gamma} p^\alpha k^\beta p'^\gamma + \tfrac{1}{2} k\cdot p\, g_{\rho\sigma} \varepsilon_{\nu\mu\alpha\beta} k^\alpha p'^\beta$$

$$Y^1_{\mu\nu\rho\sigma} = 2k\cdot p' p_\nu p_\sigma g_{\mu\rho} - 2p\cdot p' p_\nu k_\sigma g_{\mu\rho} - 2p'_\mu p_\nu k_\rho p_\sigma + k\cdot p k\cdot p' g_{\mu\rho} g_{\nu\sigma} - 2k\cdot p\, p'_\nu k_\sigma g_{\mu\rho}$$

$$Y^2_{\mu\nu\rho\sigma} = k\cdot p\, p_\mu \varepsilon_{\nu\rho\alpha\sigma} p'^\alpha - p_\mu p_\nu \varepsilon_{\alpha\rho\beta\sigma} q'^\alpha q'^\beta$$

$$\begin{aligned} X^3_{\mu\nu\rho\sigma} = {} & p'\cdot k\,(3g_{\mu\nu} k_\rho p_\sigma + 2p_\mu k_\sigma g_{\nu\rho} - 2p_\sigma p_\mu g_{\nu\rho} + p_\mu p_\nu g_{\rho\sigma} - p_\mu p'_\nu g_{\rho\sigma} - p\cdot k\, g_{\mu\nu} g_{\rho\sigma}) \\ & + p_\mu k\,(-g_{\mu\nu} k_\rho p'_\sigma + 2p'_\mu k_\sigma g_{\nu\rho} - 2p'_\nu p'_\rho g_{\mu\sigma} + 2p'_\rho p_\mu g_{\nu\sigma} + p'_\mu p'_\nu g_{\rho\sigma} + p_\mu p'_\nu g_{\rho\sigma}) \\ & + p\cdot p'\,(g_{\mu\nu} k_\rho k_\sigma + 2p_\mu p'_\nu g_{\rho\sigma}) - 2p_\mu p'_\nu k_\rho k_\sigma + 2p_\mu p'_\nu p'_\rho k_\sigma + 2p_\mu p'_\nu k_\rho p_\sigma - p_\mu p'_\nu p_\rho p'_\sigma \end{aligned}$$

$$\begin{aligned} X^4_{\mu\nu\rho\sigma} = {} & -k_\rho p_\sigma \varepsilon_{\mu\alpha\nu\beta} p'^\alpha k^\beta + k_\rho \varepsilon_{\alpha\beta\nu\gamma} p^\alpha p'^\beta k^\gamma g_{\mu\sigma} - p_\mu \varepsilon_{\alpha\beta\nu\gamma} p^\alpha p'^\beta k^\gamma g_{\rho\sigma} - k_\rho p'_\nu \varepsilon_{\sigma\alpha\mu\beta} p^\alpha k^\beta \\ & - k_\rho p_\mu \varepsilon_{\sigma\alpha\nu\beta} p'^\alpha k^\beta + 2p_\sigma p_\mu \varepsilon_{\rho\alpha\nu\beta} p'^\alpha k^\beta + k\cdot p' p_\sigma \varepsilon_{\mu\rho\nu\alpha} k^\alpha + p_\sigma p'_\nu \varepsilon_{\mu\alpha\rho\beta} k^\alpha p'^\beta \\ & - p'_\nu \varepsilon_{\alpha\beta\rho\gamma} p^\alpha k^\beta p'^\gamma g_{\mu\sigma} + p'_\rho p'_\nu \varepsilon_{\sigma\alpha\mu\beta} p^\alpha k^\beta + k_\rho p'_\nu \varepsilon_{\sigma\alpha\mu\beta} p^\alpha p'^\beta \end{aligned}$$

$$Y^3_{\mu\nu\rho\sigma} = p'\cdot k\,(-4p_\mu k_\sigma g_{\nu\rho} - 2p'_\nu p_\sigma g_{\mu\rho} - 2p\cdot k\, g_{\mu\rho} g_{\nu\sigma}) + 2p\cdot p'\,(k_\rho p_\mu g_{\nu\sigma} - k_\rho p'_\nu g_{\mu\sigma})$$

$$\begin{aligned} Y^4_{\mu\nu\rho\sigma} = {} & k_\rho \varepsilon_{\alpha\beta\nu\gamma} p^\alpha p'^\beta k^\gamma g_{\mu\sigma} - k_\rho p'_\nu \varepsilon_{\sigma\alpha\mu\beta} p^\alpha k^\beta - k_\rho p_\mu \varepsilon_{\sigma\alpha\nu\beta} p'^\alpha k^\beta + p_\mu p'_\nu \varepsilon_{\sigma\alpha\rho\beta} p^\alpha k^\beta \\ & - 2p_\mu p'_\nu \varepsilon_{\sigma\alpha\rho\beta} p^\alpha p'^\beta + k\cdot p' p_\mu \varepsilon_{\sigma\rho\nu\alpha} k^\alpha + p_\sigma p'_\nu \varepsilon_{\mu\alpha\rho\beta} k^\alpha p'^\beta - p'_\nu \varepsilon_{\alpha\rho\beta\gamma} p^\alpha k^\beta p'^\gamma g_{\mu\sigma} \\ & + p_\rho p'_\nu \varepsilon_{\sigma\alpha\rho\beta} k^\alpha p'^\beta + p'_\sigma p'_\nu \varepsilon_{\sigma\alpha\mu\beta} p^\alpha k^\beta - k\cdot p' p'_\nu \varepsilon_{\sigma\alpha\mu\rho} p^\alpha + k_\rho p'_\nu \varepsilon_{\sigma\alpha\mu\beta} p^\alpha p'^\beta + p_\mu \varepsilon_{\sigma\rho\nu\beta} p^\alpha (-k\cdot p'). \end{aligned}$$

(D.5)

This very long expression can only be useful with the help of a computer. Nevertheless, a look at its structure is interesting. The symmetric tensor $S^{\mu\nu}$ gives the unpolarized and the photon linear polarization contributions. The antisymmetric tensor $A^{\mu\nu}$ gives the photon circular polarization contribution.

In the case of pure γ exchange ($a^2 = 1$, $b = 0$, $a_f = Q_f$, $b_f = 0$) only the SU and AΣ types of combination remain because of parity conservation. This means that circular photon polarization is always associated with $e^{\pm}$ longitudinal polarization ($\bar{\lambda} P_L$) but linear photon polarization can be analyzed without $e^{\pm}$ polarization through the orientation of the production plane $(\vec{p},\vec{p}')$ of the $f\bar{f}$ pair. In the case of Z^0 exchange, parity violating terms $(ab, a_f b_f)$ introduce different combinations (AU and SΣ) with new polarization correlations.

In the case of unpolarized incident photons this expression simplifies to:

$$
\begin{aligned}
N = {} & \left[a^2+b^2+2ab\,Q_e P_L\right]\Big\{(a_f^2+b_f^2)\left[(3m^2-q'^2)(2\ell'\cdot p'\,\ell\cdot p'+\ell\cdot\ell'(q'\cdot p'-m^2))+(m^2-q'^2)(\ell'\cdot p\,\ell\cdot p'+\ell'\cdot p'\,\ell\cdot p)\right] \\
& \qquad -(a_f^2-b_f^2)\,m^2\,\ell\cdot\ell'(m^2+q'^2)\Big\} \\
& +\left[2ab\,Q_e+P_L(a^2+b^2)\right]2a_f b_f\Big\{(3m^2-q'^2)(\ell\cdot k\,\ell'\cdot p'-\ell\cdot p'\,\ell'\cdot k')-(m^2-q'^2)(\ell\cdot p'\,\ell'\cdot p-\ell\cdot p\,\ell'\cdot p')\Big\}
\end{aligned}
$$

$$
\begin{aligned}
N'' = {} & \left[a^2+b^2+2ab\,Q_e P_L\right]\Big\{(a_f^2+b_f^2)\left[\ell\cdot\ell'(4m^4-2m^2k\cdot k'+2k'^2(p\cdot p'-m^2)-2(k'\cdot p-m^2)(2\ell'\cdot p'\,\ell\cdot p'-m^2\ell\cdot\ell')\right. \\
& \left.-2(k'\cdot p'-m^2)(2\ell\cdot p\,\ell'\cdot p-m^2\ell\cdot\ell')-(\ell'\cdot p\,\ell\cdot p'+\ell'\cdot p'\,\ell\cdot p-\ell\cdot\ell'\,p\cdot p')(4p\cdot p'-2p'\cdot k-2p\cdot k')\right] \\
& -8m^2a_f^2(\ell'\cdot p\,\ell\cdot p'+\ell'\cdot p'\,\ell\cdot p-\ell\cdot\ell'\,p\cdot p') \\
& -m^2(a_f^2-b_f^2)(2\ell\cdot\ell'(q'\cdot p'+q''\cdot p)+4\ell'\cdot p\,\ell\cdot p-4m^2\ell\cdot\ell'+4\ell'\cdot p'\,\ell\cdot p')\Big\} \\
& +\left[2ab\,Q_e+P_L(a^2+b^2)\right]4a_f b_f\Big\{p\cdot k(\ell\cdot p'\,\ell'\cdot p-\ell\cdot p\,\ell'\cdot p')-p\cdot p'(\ell\cdot k\,\ell'\cdot p-\ell\cdot p\,\ell'\cdot k) \\
& +m^2(\ell\cdot k\,\ell'\cdot p'-\ell\cdot p'\,\ell'\cdot k)-m^2(\ell\cdot k\,\ell'\cdot p-\ell\cdot p\,\ell'\cdot k)+p'\cdot k(\ell\cdot p\,\ell'\cdot p-\ell\cdot p\,\ell'\cdot p')-p\cdot p'(\ell\cdot p'\,\ell'\cdot k-\ell\cdot k\,\ell'\cdot p') \\
& +k'^2(\ell\cdot p'\,\ell'\cdot p-\ell\cdot p\,\ell'\cdot p')+m^2(\ell\cdot k'\,\ell'\cdot p-\ell\cdot p\,\ell'\cdot k'-\ell\cdot k'\,\ell'\cdot p'+\ell\cdot p'\,\ell'\cdot k')\Big\}
\end{aligned}
\tag{D.6}
$$

If we now restrict ourselves to pure γ exchange in the unpolarized case the simplest form is given by

$$N = 2(3m^2-q'^2)\ell'\cdot p'\ell\cdot p' + (m^2-q'^2)(\ell'\cdot p\,\ell\cdot p' + \ell'\cdot p'\ell\cdot p) - \ell\cdot\ell'(4m^4+q'^2q'\cdot p') \tag{D.7}$$

$$N'' = 2\Big\{-2\ell'\cdot p\ell\cdot p\,k'\cdot p' - 2\ell'\cdot p'\ell\cdot p'\,k'\cdot p - (\ell'\cdot p\,\ell\cdot p' + \ell'\cdot p'\ell\cdot p)(2m^2+k\cdot(p+p')) + \ell\cdot\ell'\big[p\cdot p'(2m^2+k'\cdot(p+p')) + m^2k'\cdot(p+p')\big]\Big\} .$$

	ν	e	u	d
$(2\sin 2\theta_W)a_f$	1	$-1+4\sin^2\theta_W$	$1-\frac{8}{3}\sin^2\theta_W$	$-1+\frac{4}{3}\sin^2\theta_W$
$(2\sin 2\theta_W)b_f$	1	-1	1	-1

Table 1: Standard $Zf\bar{f}$ coupling constants

$U(\pm\pm)=\lvert\ell'^*\rvert^2\sin^2\alpha^*+\ell\cdot\ell'$
$U(\pm\mp)=-\lvert\ell'^*\rvert^2\sin^2\alpha^*$
$U(00)=\frac{2(k'^*\ell'^{0*}-k'^{0*}\ell'^*\cos\alpha^*)^2}{-k'^2}-\ell\cdot\ell'$
$U(0\eta)=U(\eta 0)=-\frac{2\eta\ell'^*\sin\alpha^*(k'^*\ell'^{0*}-k'^{0*}\ell'^*\cos\alpha^*)}{\sqrt{-2k'^2}}$
$\Sigma(\pm\pm)=\mp(k'^*\ell'^{0*}-k'^{0*}\ell'^*\cos\alpha^*)$
$\Sigma(\pm\mp)=\Sigma(00)=0$
$\Sigma(0\eta)=\Sigma(\eta 0)=\sqrt{\frac{-k'^2}{2}}\,\ell'^*\sin\alpha^*$

Table 2: Helicity components of the leptonic vertex $L(\eta\eta')$

	π^0	η	η'	ε	f	A_2	f'	$G(\rho\rho)$	η_c	χ_c^0	χ_c^2	η_b
M(GeV)	0.14	0.55	0.96	1.3	1.27	1.31	1.51	1.65	2.97	3.41	3.55	9.4
$\Gamma_{\gamma\gamma}$(keV)	7.9×10^{-3}	0.32	5.9	10.0	5.0	1.8	0.4	8.0	6.4	1.0	0.4	0.4
σ(nb)	12.0	7.0	20.0	15.0	38.0	13.0	2.0	5.6	0.8	0.08	0.1	10^{-3}

Table 3: Single boson production cross-section $\sigma(\gamma e^{\pm} \to B^0 e^{\pm})$ in γ exchange processes

REFERENCES

1) C. Akerlof, preprint UM HE 81-59 (1981).

2) F.M. Renard, Basics of e^+e^- collisions, ed. Frontières (1981).

3) V.M. Budnev et al., Phys. Rep. 15C (1975) 181;
H. Terazawa, Rev. Mod. Phys. 45 (1973) 615.

4) Proc. Int. $\gamma\gamma$ Coll. Paris 1973: Phys. Suppl. 35, C2 (1974) 1;
Proc. Int. $\gamma\gamma$ Coll. Lake Tahoe, ed. J.F. Gunion (1979);
Proc. Int. $\gamma\gamma$ Workshop Amiens, eds. G. Cochard and P. Kessler (Springer Verlag) (1980);
Proc. 4th Int. $\gamma\gamma$ Coll. Paris, ed. G.W. London (1981).

5) Physics with very high energy e^+e^- colliding beams, CERN 76/18 (1976);
Proc. of LEP Summer Study, Les Houches and CERN, CERN 79/01 (1979);
ECFA-LEP Working Group 79 progress report, ECFA 79/39 (1979).

6) O. Klein and Y. Nishina, Z. Physik 52 (1929) 853.

7) J.A. McClure and S.D. Drell, Nuovo Cimento 37 (1965) 1638.

8) N.M. Kroll, Nuovo Cimento 45 (1966) 65.

9) R. Hollebeek, J. Bürger and J.G. Branson, Int. Symp. Lepton Photon, Bonn, ed. W. Pfeil (1981).

10) M. Capdequi Peyranère et al., Nucl. Phys. B149 (1979) 243.

11) F.E. Low, Phys. Rev. Lett. 14 (1965) 238.

12) H.A. Bethe and W. Heitler, Proc. Roy. Soc. Lond. A146 (1934) 86.

13) F.A. Berends, K.J.F. Gaemers and R. Gastmans, Nucl. Phys. B61 (1973) 414.

14) F.M. Renard, Nucl. Phys. B196 (1982) 83.

15) K.O. Mikaelian, Phys. Rev. D17 (1978) 750.

16) J. Prentki and G. Preparata, unpublished.

17) A. Donnachie and K.J.F. Gaemers, Z. Physik C4 (1980) 37.

18) W.A. Bardeen, Int. Symp. Lepton Photon, Bonn, ed. W. Pfeil (1981).

19) J. Ellis, Lectures at Les Houches, LAPP-TH-48 (CERN TH-3174) (1981).

20) P. Fayet, Proc. ESC Conf, Erice, ed. Plenum Pub. Corp. (1980); talk given at XVI Rencontre de Moriond, QCD and Lepton Physics, ed. Frontières (1981).

21) R. Barbieri et al., CERN preprint TH-3089 (1981);
H. Fritzsch, CERN preprint TH-3219 (1981) and references therein.

22) J. Bürger, Int. Symp. Lepton Photon, Bonn, ed. W. Pfeil (1981).

FIGURE CAPTIONS

Fig. 1: Quasi-real $\gamma e^{\pm}$ collisions in e^+e^- inelastic scattering.

Fig. 2: γ-e collision c.m. frame.

Fig. 3: Compton scattering $\gamma e^{\pm} \to \gamma e^{\pm}$.

Fig. 4: Seagull term for anomalous Compton scattering.

Fig. 5: Excited (e^*) electron contributions to Compton scattering.

Fig. 6: Contributions to lepton pair production
a) boson exchange terms
b) Compton-like terms.

Fig. 7: Diagrams for $\gamma e \to Ze$.

Fig. 8: Angular distribution of $\gamma e \to Ze$ at $\sqrt{s}$ = 100 GeV.

Fig. 9: Integrated cross-section $\sigma(\gamma e \to Ze)$.

Fig. 10: Diagrams for $\gamma e^{\pm} \to W^{\pm}\nu_e$.

Fig. 11: Angular distribution of $\gamma e^{\pm} \to W^{\pm}\nu_e$ at $\sqrt{s}$ = 100 GeV.

Fig. 12: Integrated cross-section $\sigma(\gamma e^{\pm} \to W^{\pm}\nu_e)$.

Fig. 13: Boson exchange diagram for $\gamma e \to (B) + (F)$.

Fig. 14: $\gamma\gamma$ luminosity factor $K(s,W)$ for γe collisions.

Fig. 15: Boson exchange diagram for $\gamma e \to (B) + (F)$.

Fig. 16: Diagrams for $\gamma\gamma \to B^+B^-$ (spin zero pair).

Fig. 17: $d\sigma/dx$ for spin zero pair production at $\sqrt{s}$ = 100 GeV.

Fig. 18: Diagrams for $\gamma\gamma \to f\bar{f}$ (fermion pair).

Fig. 19: $d\sigma/dx$ for fermion pair production at $\sqrt{s}$ = 100 GeV.

Fig. 20: Diagrams for $\gamma e^{\pm} \to B^0 f^{\pm}$.

Fig. 21: cross-sections for $\gamma e^{\pm} \to B^0 f^{\pm}$:
——— $f^{\pm} \equiv e^{\pm}$ and m_{B^0} = 10, 20 or 40 GeV,
------- $f^{\pm} \neq e^{\pm}$, m_f = 40 GeV and m_{B^0} = 10, 20 or 40 GeV.

Fig. 22: Diagrams for $\gamma e^{\pm} \to B^{\pm} + f^0$.

Fig. 23: Cross-sections for $\gamma e^{\pm} \to B^{\pm} + f^0$:
——— $f^0 \equiv \nu_e$ and m_B = 10, 20 or 40 GeV,
------- $f^0 \neq \nu_e$, m_f = 40 GeV and m_B = 10, 20 or 40 GeV.

Fig. 24: New fermion formation process.

Fig. 25: Diagram for $\gamma e \to f \to B + f'$.

Fig. 26: Diagram for $\gamma e \to B + F$ through f exchange.

Fig. 27: Diagram for scalar boson exchange.

Fig. 28: Reference frames
a) in γ-e c.m.,
b) in γ-b c.m. (for b exchange processes).

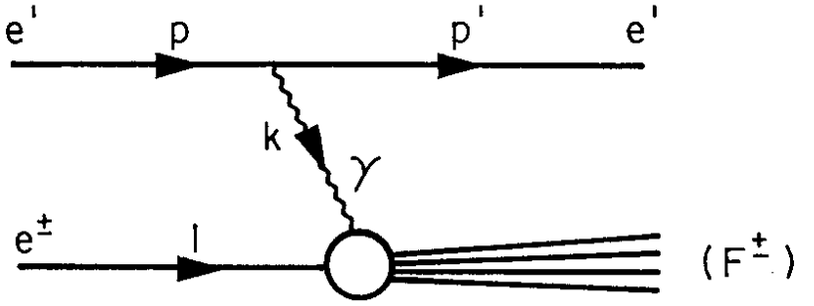

Fig. 1

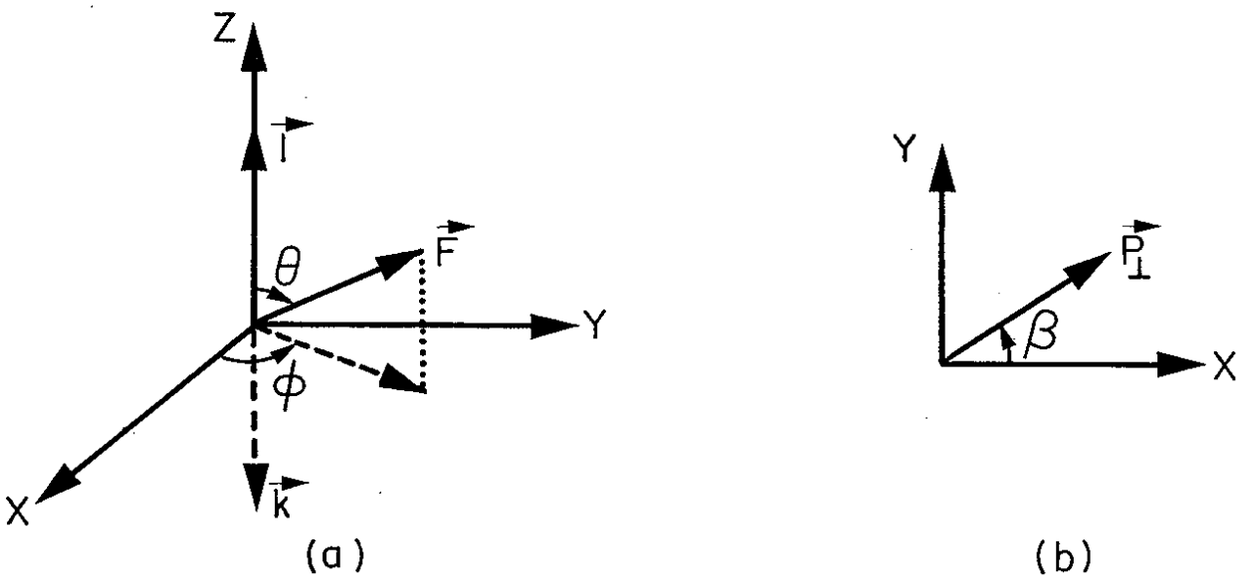

Fig. 2

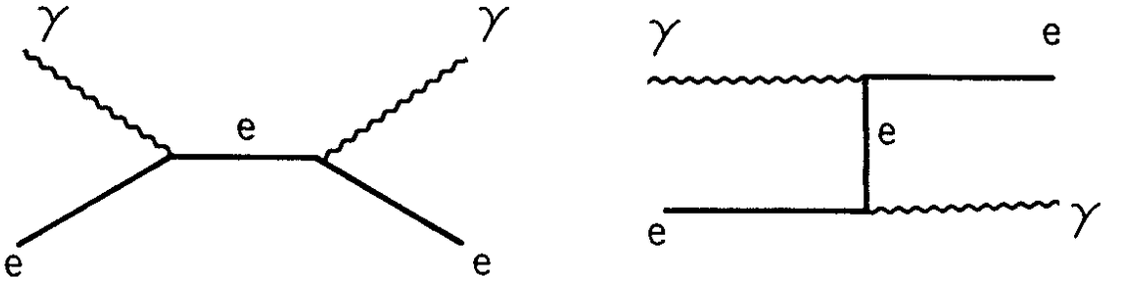

Fig. 3

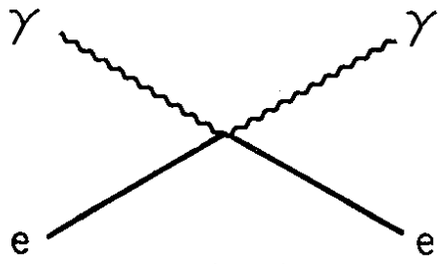

Fig. 4

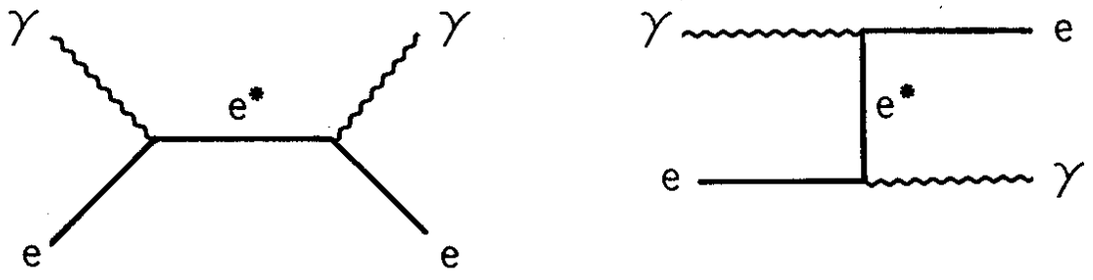

Fig 5

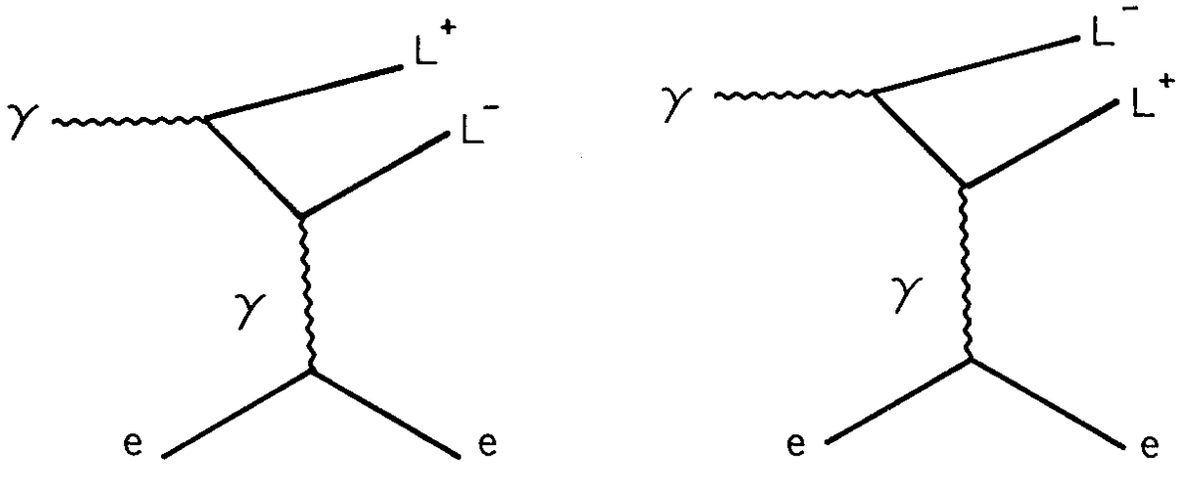

Fig. 6a

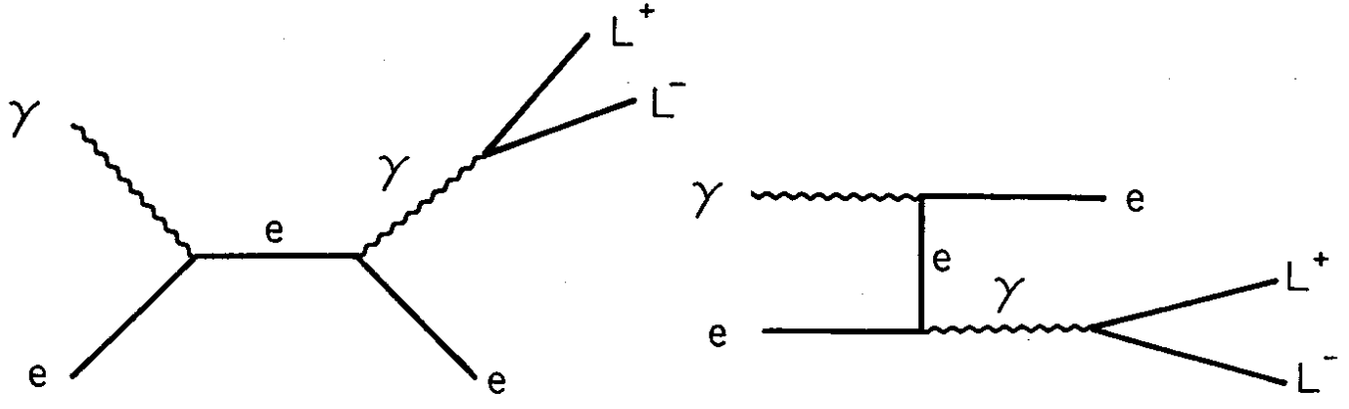

Fig. 6b

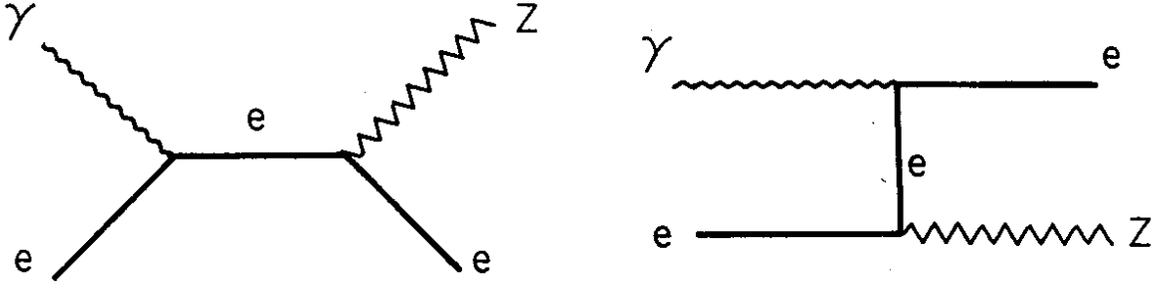

Fig. 7

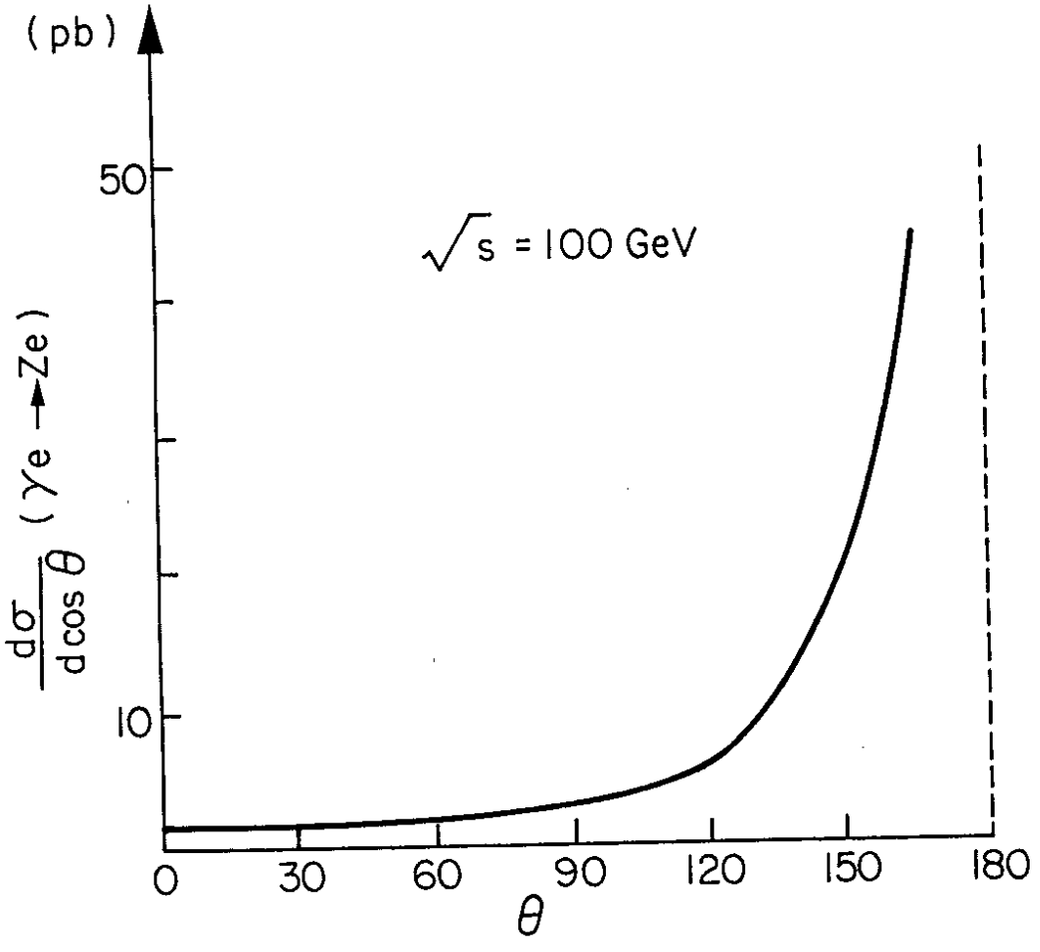
(pb)
50
10
$\frac{d\sigma}{d\cos\theta}(\gamma e \to Ze)$
$\sqrt{s}$ = 100 GeV
0
30
60
90
120
150
180
θ

Fig. 8

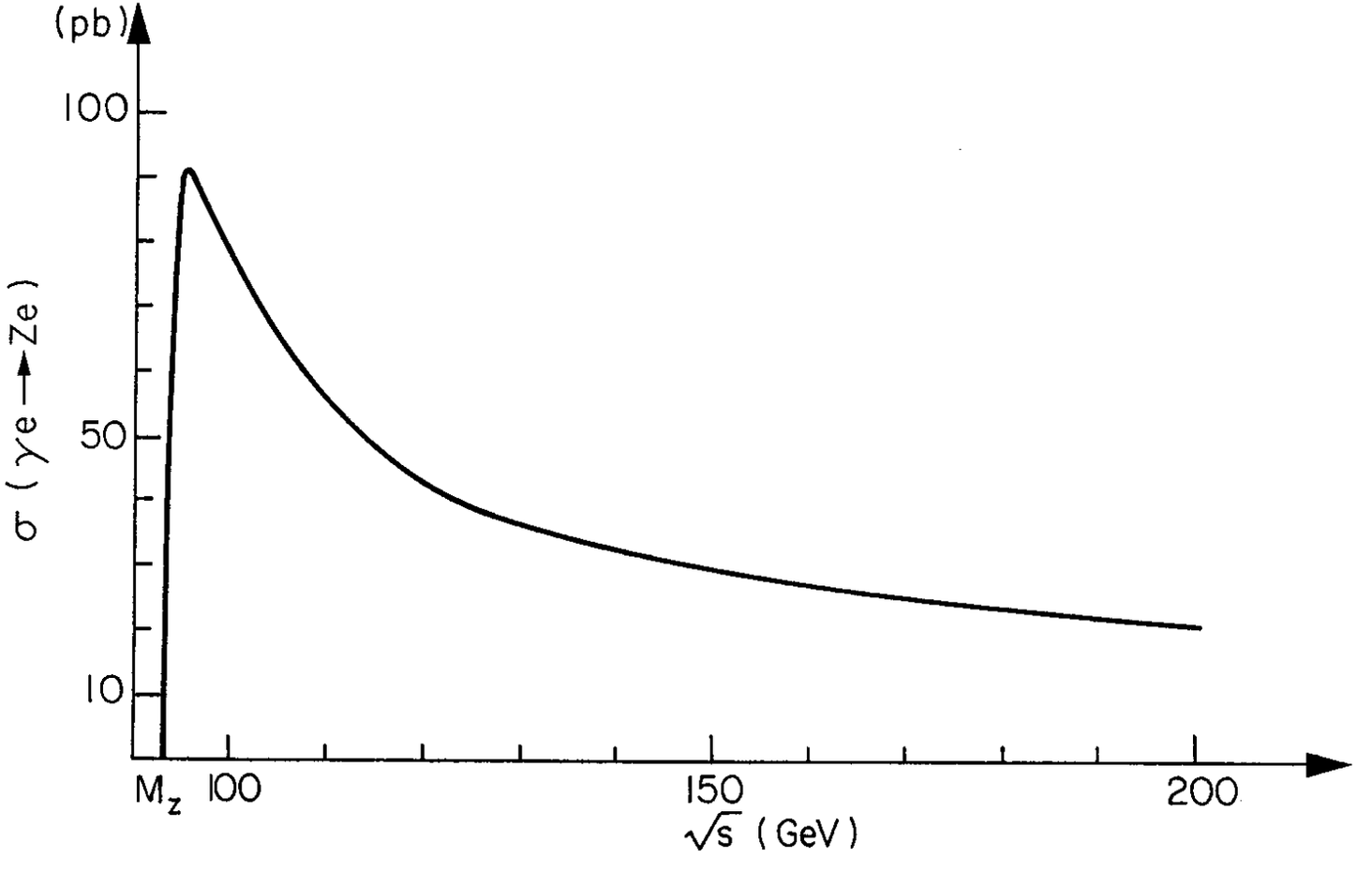

Fig.9

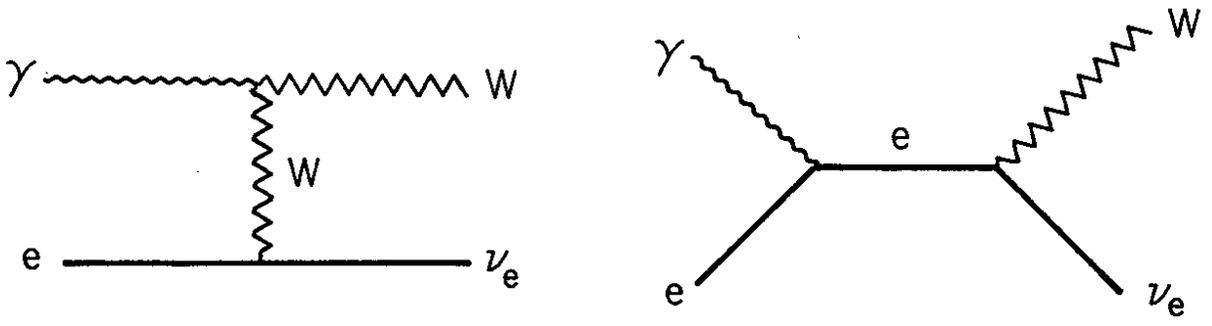
γ
W
W
e
ν_e
γ
W
e
e
ν_e

Fig. 10

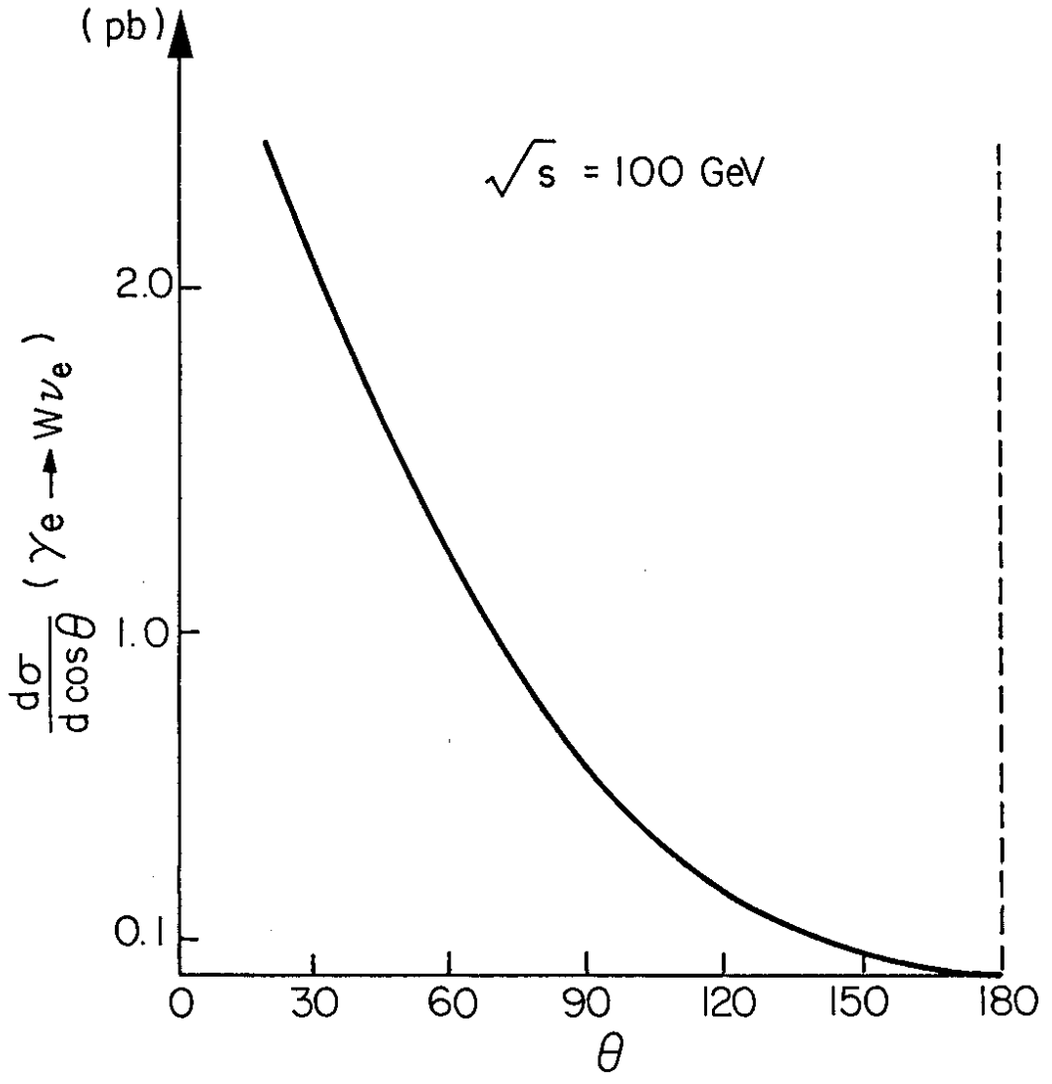
(pb)
$\sqrt{s}$ = 100 GeV
$\frac{d\sigma}{d\cos\theta}(\gamma e \to W\nu_e)$
2.0
1.0
0.1
0
30
60
90
120
150
180
θ

Fig. 11

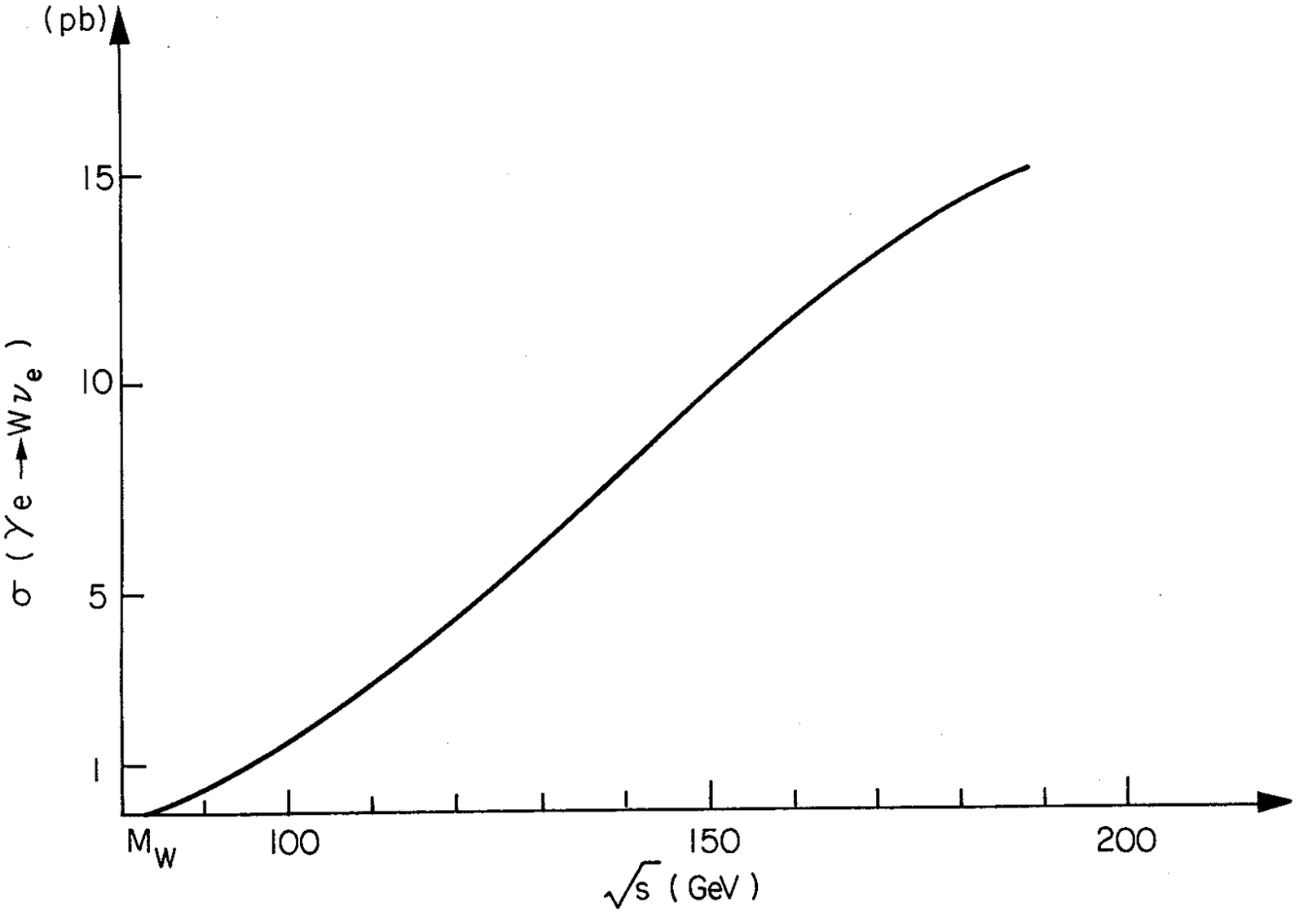

Fig. 12

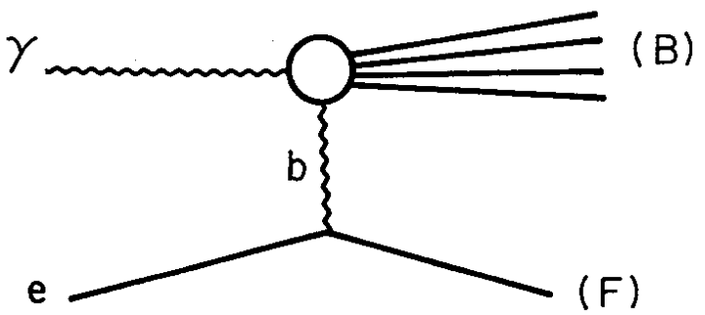

Fig. 13

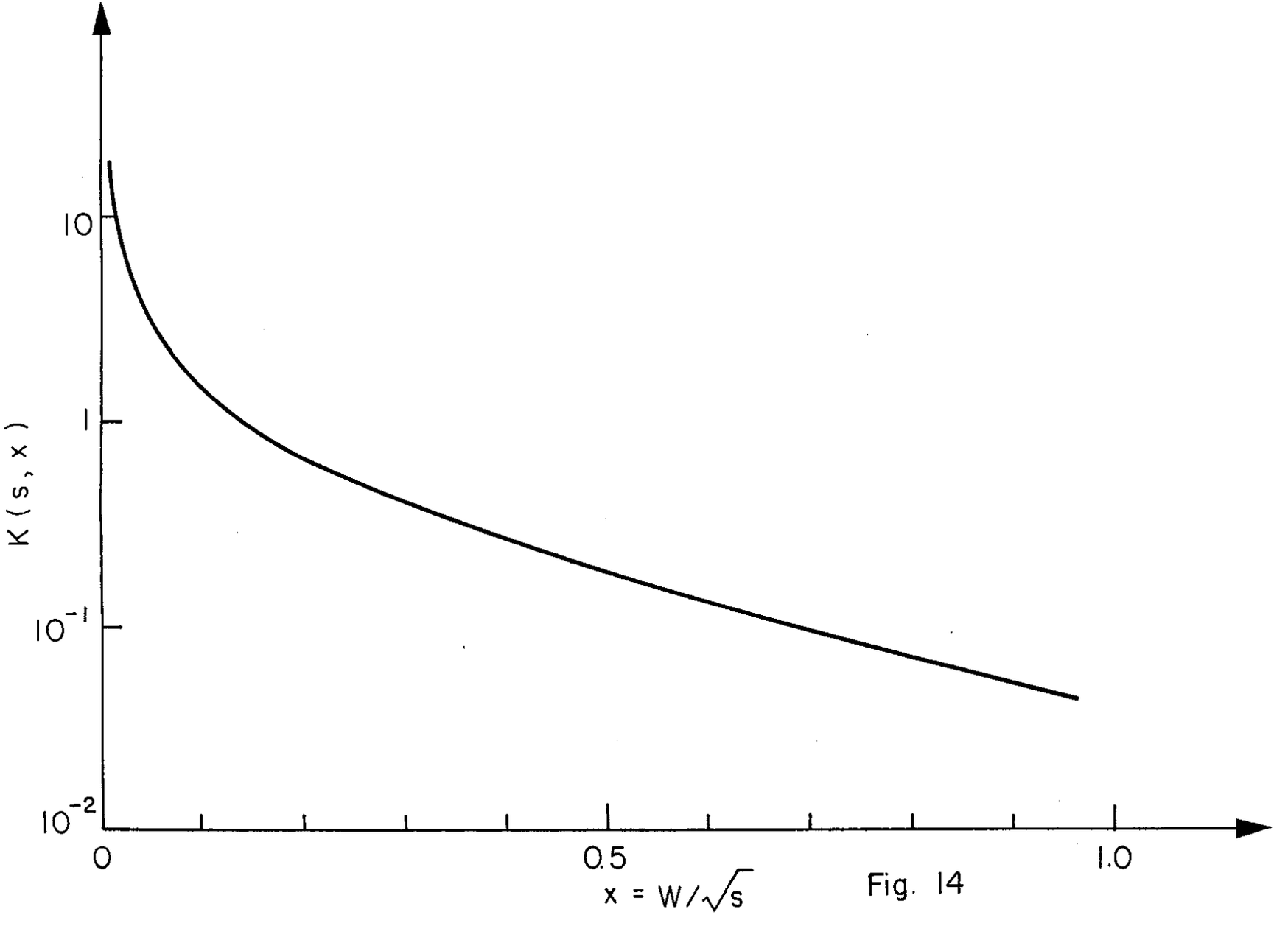

Fig. 14

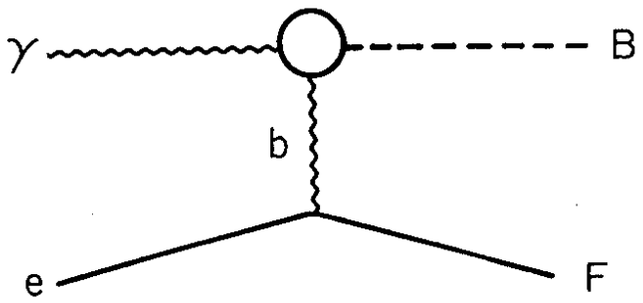

Fig. 15

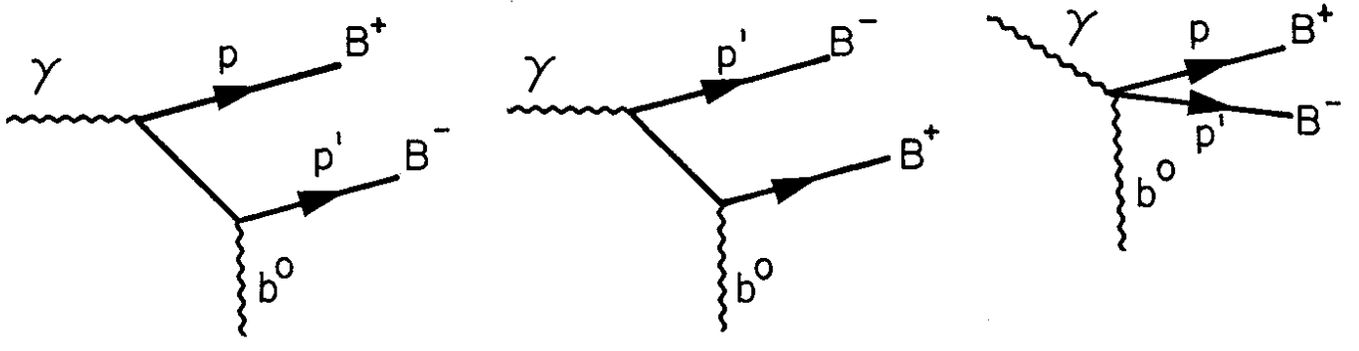

Fig. 16

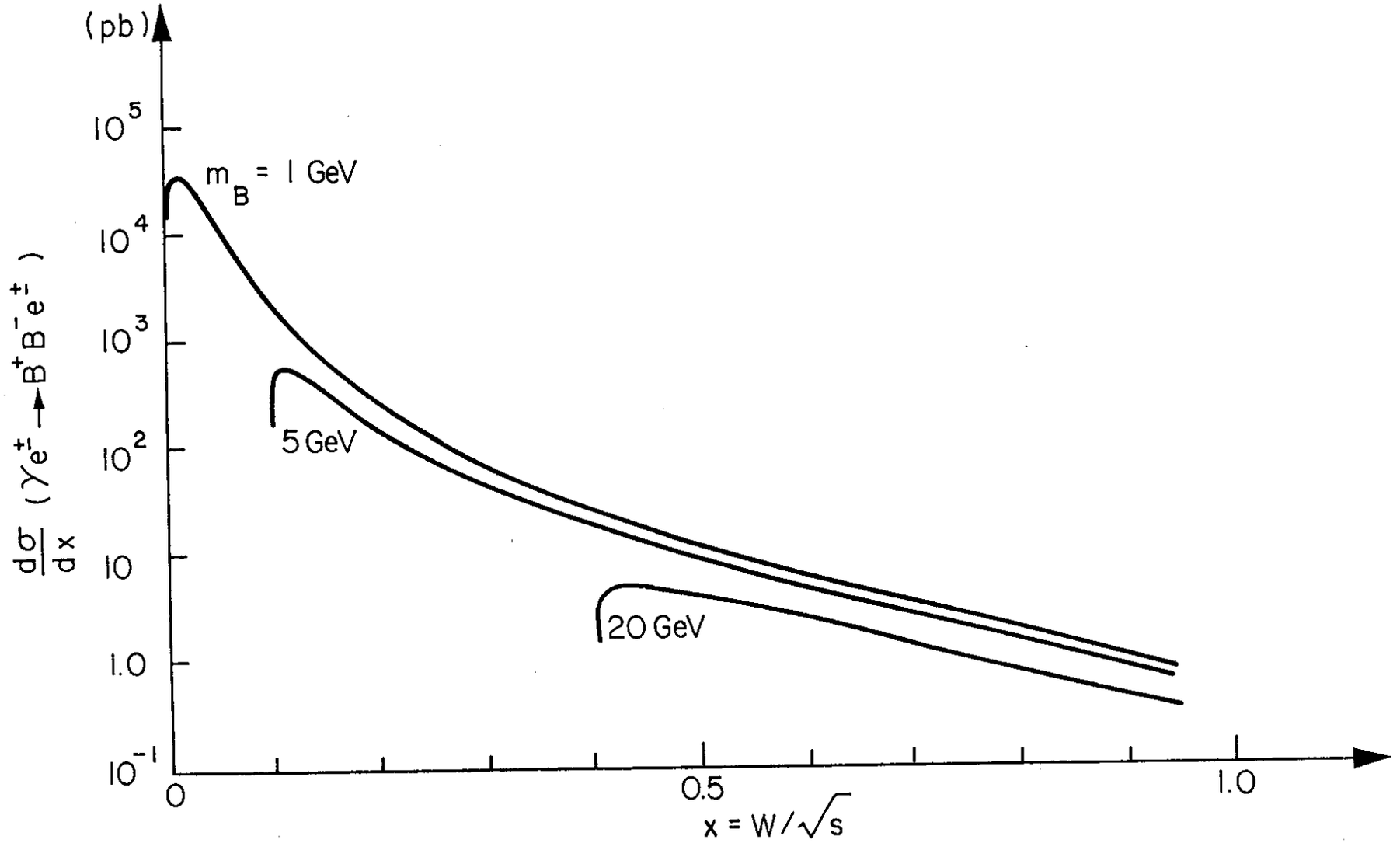
(pb)
10^5
10^4
10^3
10^2
10
1.0
10^{-1}
m_B = 1 GeV
5 GeV
20 GeV
$\frac{d\sigma}{dx}$ ($\gamma e^{\pm} \rightarrow B^+ B^- e^{\pm}$)
0
0.5
1.0
$x = W/\sqrt{s}$

Fig. 17

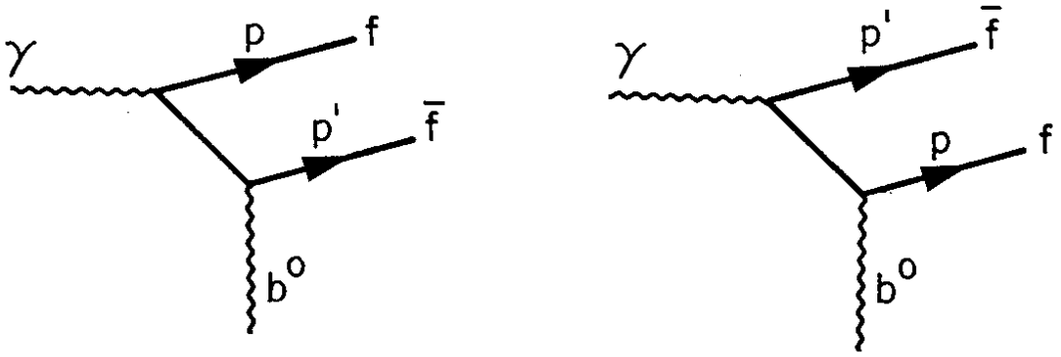

Fig. 18

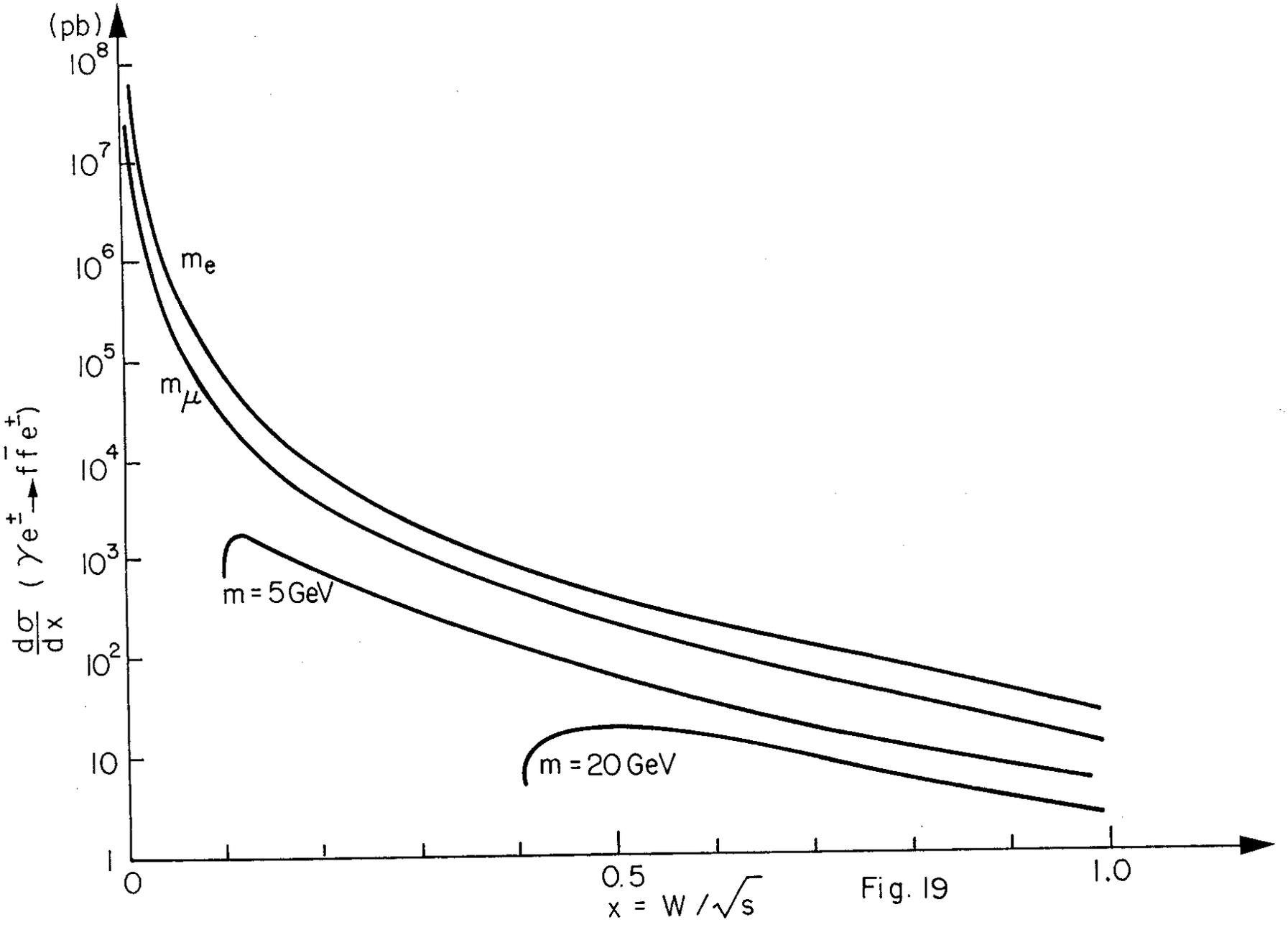
(pb)
10^8
10^7
10^6
10^5
10^4
10^3
10^2
10
1
m_e
m_μ
m = 5 GeV
m = 20 GeV
$\frac{d\sigma}{dx}$ ($\gamma e^{\pm} \rightarrow f \bar{f} e^{\pm}$)
0
0.5
1.0
$x = W/\sqrt{s}$

Fig. 19

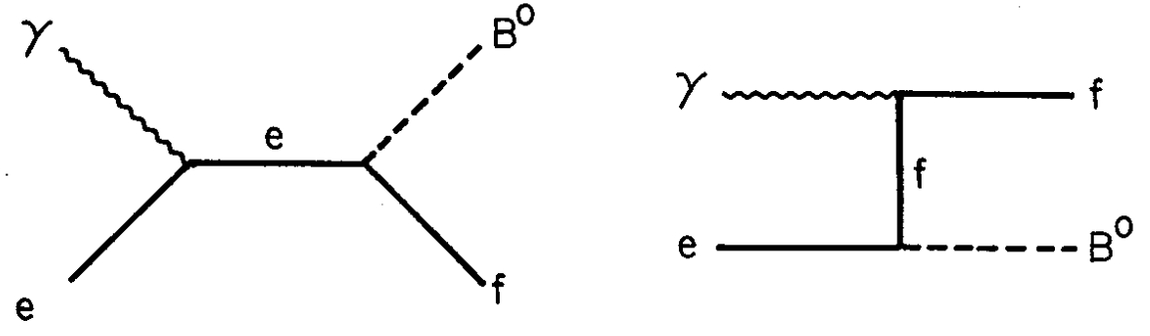

Fig. 20

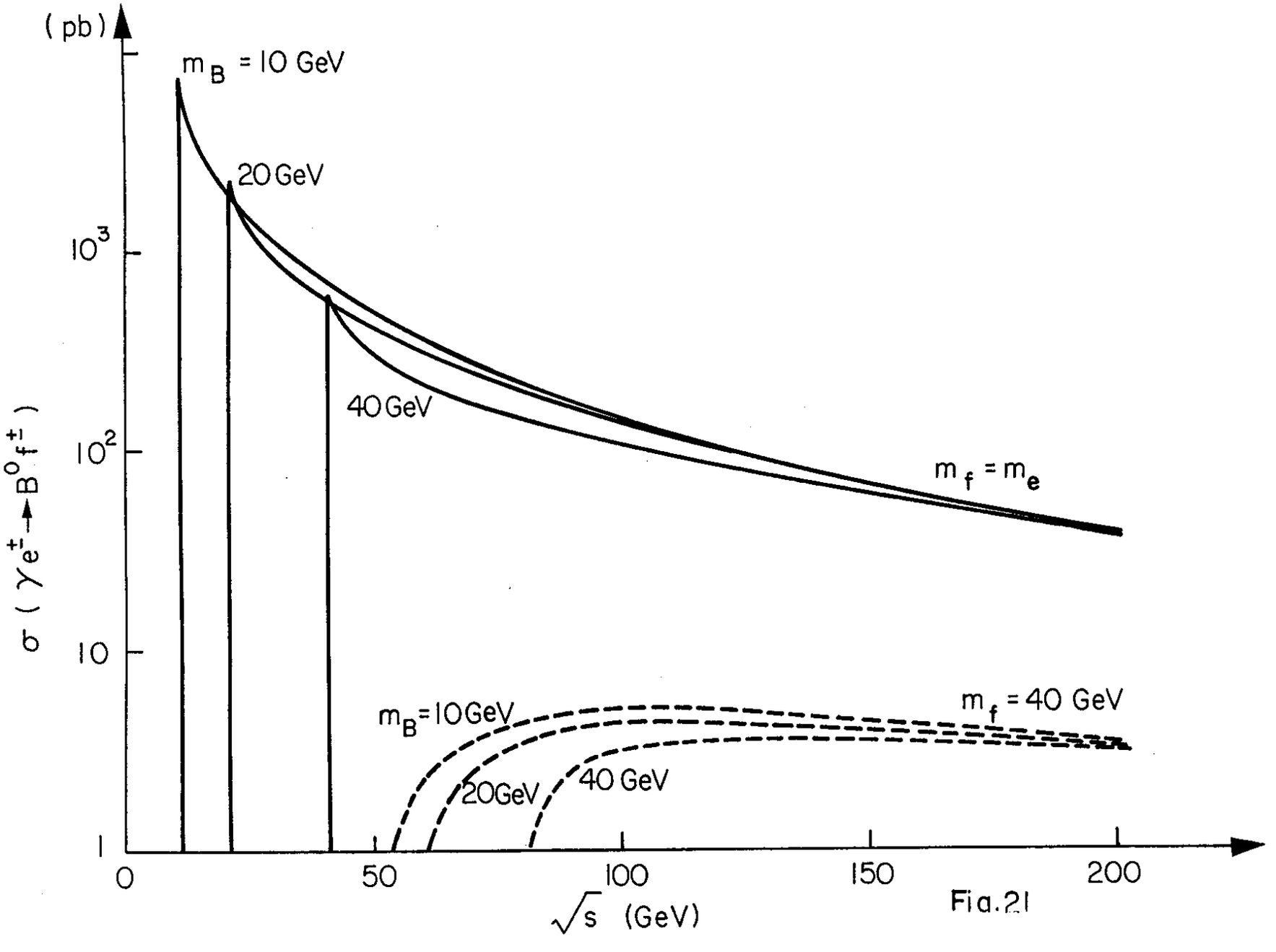
(pb)
m_B = 10 GeV
20 GeV
40 GeV
$m_f = m_e$
m_B=10GeV
m_f = 40 GeV
20GeV
40 GeV
10^3
10^2
10
1
0
50
100
150
200
$\sqrt{s}$ (GeV)
$\sigma (\gamma e^{\pm} \rightarrow B^0 f^{\pm})$

Fig.21

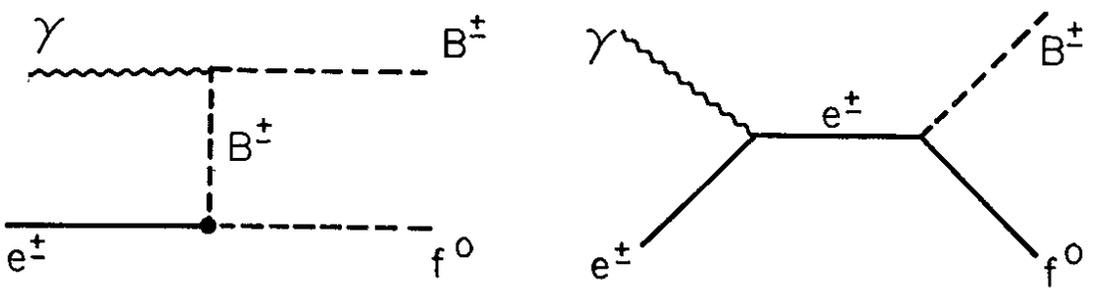

Fig. 22

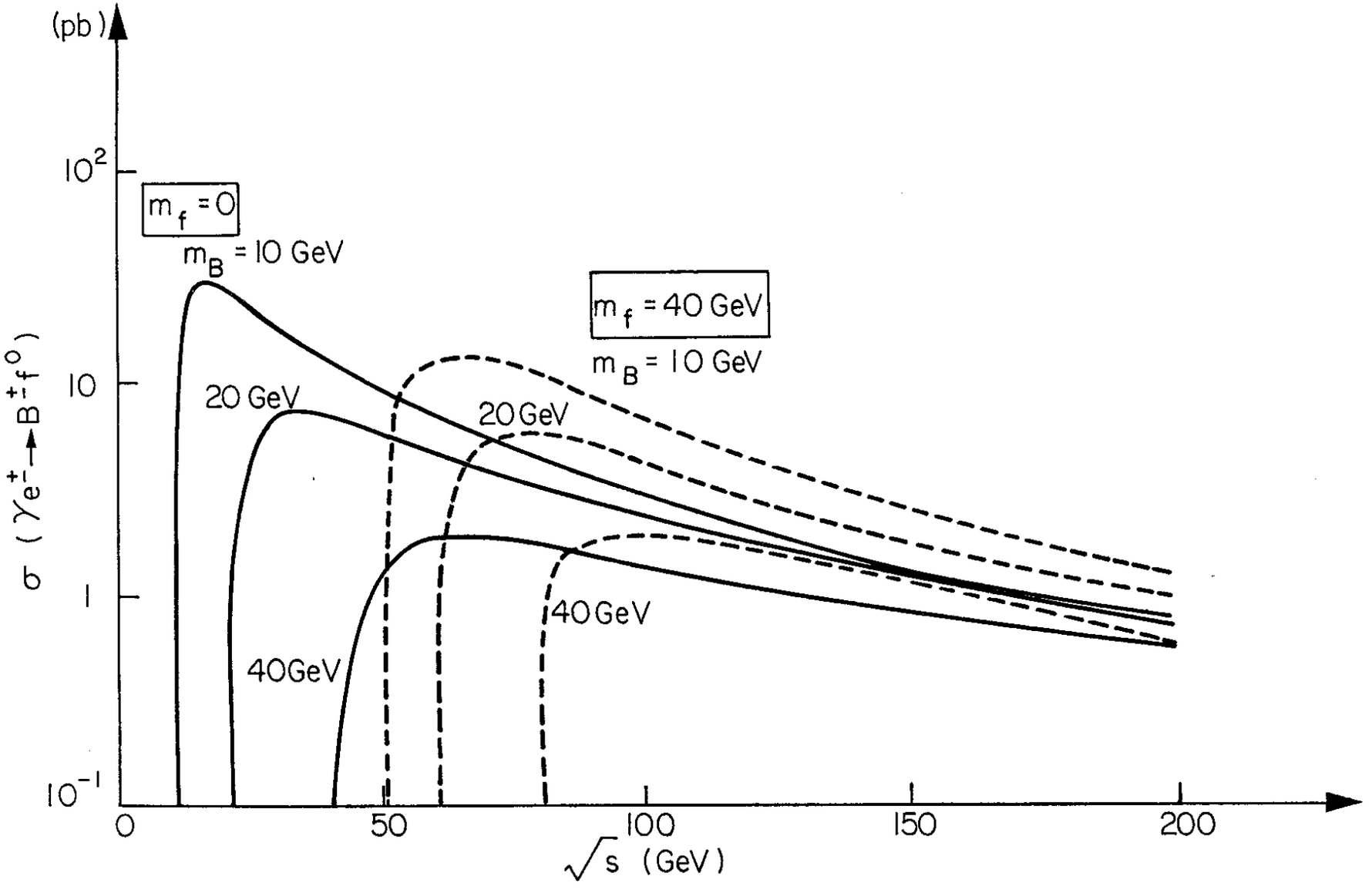
(pb)
10^2
10
1
10^{-1}
$\sigma(\gamma e^{\pm} \to B^{\pm} f^0)$
$m_f = 0$
$m_B = 10$ GeV
20 GeV
40GeV
$m_f = 40$ GeV
$m_B = 10$ GeV
20 GeV
40 GeV
0
50
100
150
200
$\sqrt{s}$ (GeV)

Fig.23

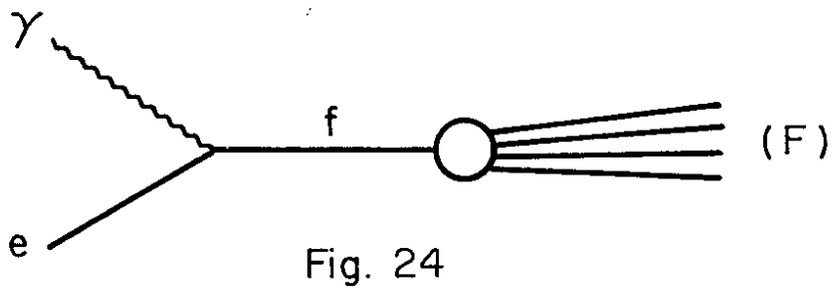

Fig. 24

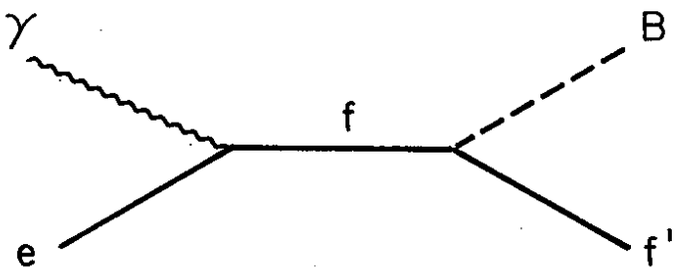

Fig. 25

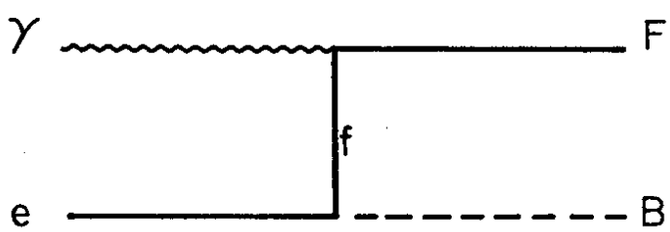

Fig. 26

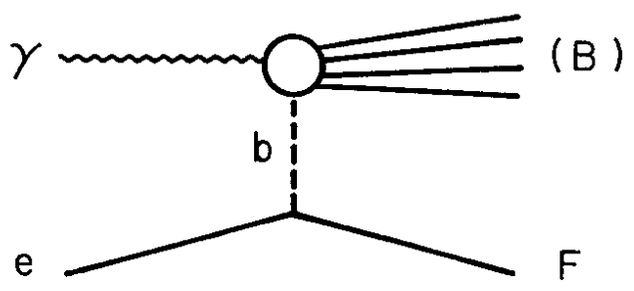

Fig. 27

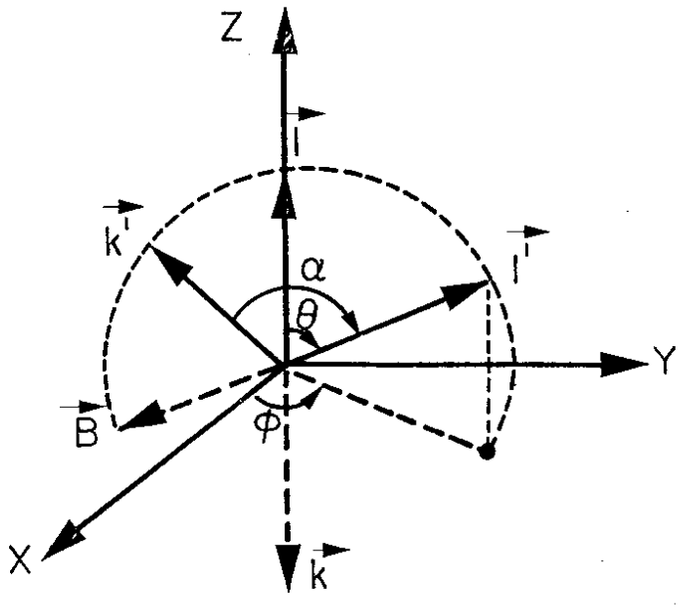

(a)

Fig. 28

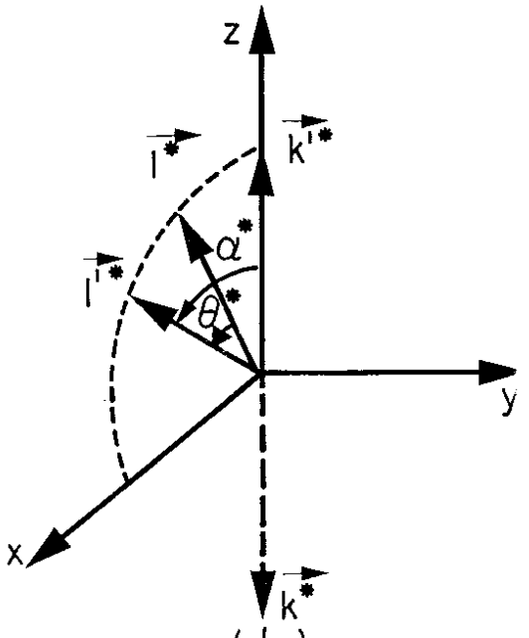

(b)